NASA-OAI COLLABORATIVE AEROSPACE RESEARCH AND FELLOWSHIP PROGRAM

AT

NASA GLENN RESEARCH CENTER

AT LEWIS FIELD

CLEVELAND, OHIO

PREPARED BY THE CO-DIRECTORS:

ANN O. HEYWARD
VICE PRESIDENT, WORKFORCE ENHANCEMENT
OHIO AEROSPACE INSTITUTE

FRANCIS J. MONTEGANI
UNIVERSITY AFFAIRS OFFICER
NASA GLENN RESEARCH CENTER

CONTENTS

INTRODUCTION

During the summer of 2002, a 10-week activity for university faculty entitled the NASA-OAI Collaborative Aerospace Research and Fellowship Program (CFP) was conducted at the NASA Glenn Research Center in collaboration with the Ohio Aerospace Institute (OAI). This is a companion program to the highly successful NASA Faculty Fellowship Program and its predecessor, the NASA-ASEE Summer Faculty Fellowship Program, that operated for 38 years at Glenn. The objectives of CFP parallel those of its companion, viz.,

(1) to further the professional knowledge of qualified engineering and science faculty,
(2) to stimulate an exchange of ideas between teaching participants and employees of NASA,
(3) to enrich and refresh the research and teaching activities of participants' institutions, and
(4) to contribute to the research objectives of Glenn.

However, CFP, unlike the NASA program, permits faculty to be in residence for more than two summers and does not limit participation to United States citizens. Selected fellows spend 10 weeks at Glenn working on research problems in collaboration with NASA colleagues and participating in related activities of the NASA-ASEE program.

This year's program began officially on June 3, 2002 and continued through August 9, 2002. Several fellows had program dates that differed from the official dates because university schedules vary and because some of the summer research projects warranted a time extension beyond the 10 weeks for satisfactory completion of the work. The stipend paid to the fellows was $1200 per week and a relocation allowance of $1000 was paid to those living outside a 50-mile radius of the Center.

In post-program surveys from this and previous years, the faculty cited numerous instances where participation in the program has led to new courses, new research projects, new laboratory experiments, and grants from NASA to continue the work initiated during the summer. Many of the fellows mentioned amplifying material, both in undergraduate and graduate courses, on the basis of the summer's experience at Glenn. A number of 2002 fellows indicated that proposals to NASA will grow out of their summer research projects and that they intend to pursue research at their home institutions on projects related to their summer efforts. In addition, some journal articles and NASA publications will result from this past summer's activities. Fellows from past summers continue to send reprints of articles that resulted from work initiated at Glenn.

This report is intended primarily to summarize the research activities comprising the 2002 CFP Program at Glenn.

RESEARCH SUMMARIES

Brief summaries of the fellows' research assignments follow. As is clear from the reports, some of the work is of sufficient importance and content to warrant reporting in the technical literature.

Name: **H. Mike Cheung**
Education: Ph.D., Chemical Engineering
Case Western Reserve University

Permanent Position: Professor, Chemical Engineering
The University of Akron

Host Organization: Instrumentation and Controls Division
Colleague: 5520/Mark P. Wernet

Assignment:

Continue the development of a Monte-Carlo simulation of a Doppler Global Velocimetry (DGV) optical system starting with the Mie scattering from the particles in the fluid to the collection optics, through the beamsplitter, Iodine absorption cell and finally to the CCD sensor. The simulation program will read in a configuration file that completely describes the attributes of a DGV system (optical, physical layout, location of detectors, laser properties, CCD sensor noise characteristics...). The simulation program will output a set of images that simulate the data collected from a DGV system. NASA GRC has the DGV software developed at NASA Langley and this simulation program will prove invaluable for determining the accuracy of the DGV technique and provide insight into optimizing the data reduction techniques. The DGV simulation software will also prove valuable in a DDF funded projected entitled Planar Particle Imaging Doppler Velocimetry (PPIDV), which was recently awarded in March 2002.

Research Summary Submitted by Fellow:

Computer Simulation of a Digital Global Velocimeter

Digital global velocimetry (DGV) utilizes a pair of CCD cameras to probe the each velocity component of a cloud of particles illuminated by a laser. Three such camera pairs are required to fully resolve all three velocity components. The system is arranged so that both cameras are imaging the same spatial region, but one of the cameras is viewing through an iodine cell. The iodine cell transmits the scattered laser light but in a wavelength selective fashion. Thus, the intensity of the image for a given particle depends not only on the scattering properties of the particle, but on its' velocity also. The Doppler shift changes the wavelength, λ, of the scattered light depending on the velocity vector, $\vec{V}$, of the particle and the geometry of the optical system. The Doppler shift in frequency form is given by $\partial\nu = \frac{(\vec{a}-\vec{I})\cdot\vec{V}}{\lambda}$. Here $\vec{I}$ is the incident laser illumination vector and in the coordinate system I'm using will be (+1,0,0) and $\vec{a}$ is vector describing the receiving optics axis which will depend on θ and φ. Here θ is the scattering angle as it is usually defined in light scattering experiments. It has the value zero when viewing the scattering volume along the laser axis (and towards it). The other angle, φ, ranges from $-\pi/2$ to $\pi/2$ and measures the deviation of the viewing

axis from horizontal. The vector describing the receiving direction, $\bar{a}$, can be expressed in either (x,y,z) form or as a (θ,φ) pair. The two forms are related as follows:

$$r_{xz} = |\bar{a}|\cos\varphi = \cos\varphi \text{ since } |\bar{a}| \equiv 1 \qquad -\pi/2 \le \varphi \le \pi/2$$

$$x = r_{xz}\cos\theta = \cos\varphi\cos\theta \qquad -\pi \le \theta \le \pi$$

$$y = \sin\varphi$$

$$z = -\sin\theta$$

so

$$\bar{a} = (\cos\varphi\cos\theta, \sin\varphi, \sin\theta)$$

The code developed this summer takes user input of the characteristics of the particle cloud and the optical system and uses this information to compute the expected images in the reference and signal cameras. The signal camera is the one viewing the scattering volume through the wavelength sensitive iodine cell. This is accomplished by computed the electric field contribution from each particle at the lens plane of the receiving optics using Mie scattering theory. The e-field intensities for each particle are adjusted for the signal camera image based on the transmission characteristics of the iodine cell for the Doppler shifted wavelength of the light scattered from the particle. This e-field is then propagated through receiving optics via a fast Fourier transform. Since it is necessary to use many more points for the FFT calculation than are present in the CCD camera as pixels, the CCD plane image is downsampled to the resolution of the camera (typically 1024 by 1024 pixels). To make the code computationally efficient the object space (scattering volume) is imaged in small patches and the CCD image built up by downsampling and combining these small patches. For typical optical parameters a 65536 by 65536 double complex array would be required to hold the e-field from all of object space. This is a prohibitively large array to process efficiently so a much smaller array is used, typically from 64 to 1024 elements square. The typical error incurred by using the smaller arrays is on the order of

Figure 1 shows a test pattern viewed at $\theta = 105^\circ$ and $\varphi = 15^\circ$. The test pattern is composed of 227 particles of radius 1 micron and with the scattering properties of water. The test pattern was chosen to illustrate the 3 dimensional nature of the simulated images. It is being viewed from slightly "behind and above" relative to a straight side on view.

In practice a random distribution of particles is used with particle characteristics and velocities set by the user. The code creates 4 images total, 2 sets of 2 images for each camera. One of the images is computed for perpendicular polarization and the other for parallel polarization of the illuminating laser. To simulate a three component DGV system the code would be run three times with appropriate optical parameters for the three camera pairs.

This is a computationally intensive problem with the code requiring approximately 100 hours to compute the four images described for a typical 30,000 particle ensemble on a 2GHz Athlon based computer.

Figure 1 Image of a test pattern computed using the DGV simulation code viewed from theta = 105 degrees and phi = 15 degrees.

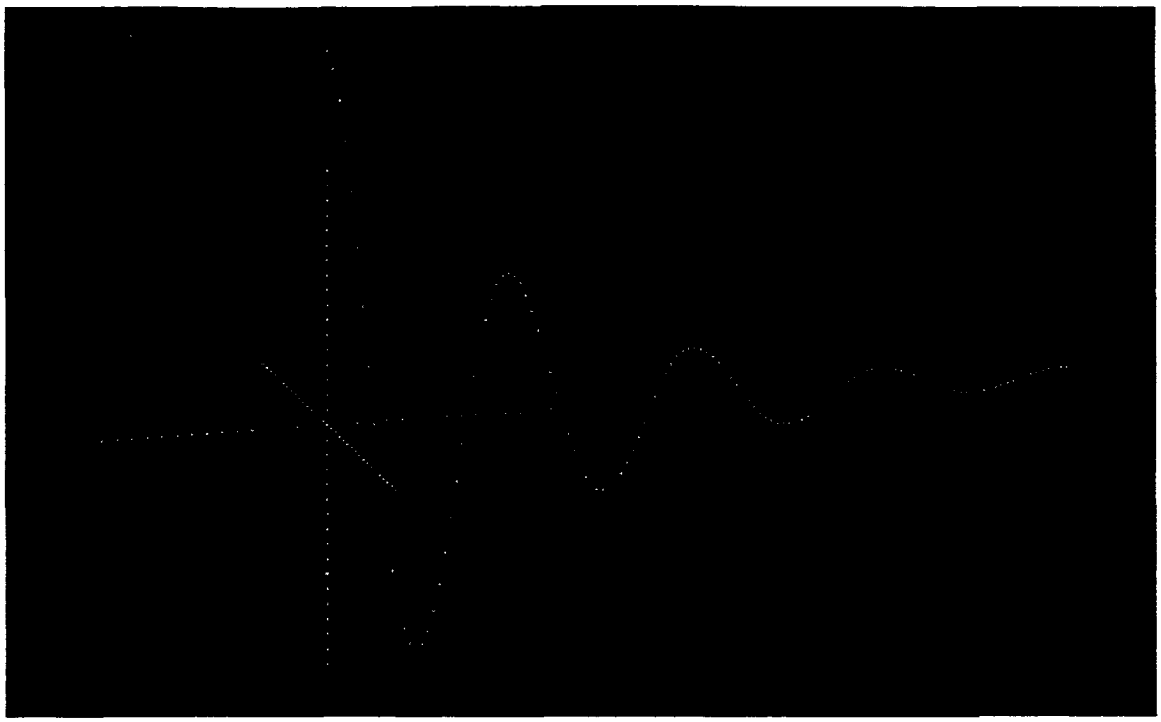

Name:	**Loren H. Dill**
Education:	Ph.D., Chemical Engineering University of Rochester
Permanent Position:	Visiting Assistant Professor, Mathematics University of Akron
Host Organization:	Microgravity Science Division
Colleagues:	Turbomachinery and Propulsion Systems Division 6727/Arnon Chait 5840/Yung K. Choo

Assignment:

During the first five-week period, Professor Dill will investigate "the effects of gravity upon the swimming direction of flagellated algae" with Dr. Arnon Chait of the Microgravity Science Division.

During the remaining five-week period, Professor Dill will evaluate "numerical grid quality control" technologies and software routines for icing aerodynamic simulation with Yung Choo, and will present the best routines with their necessary improvements to the Icing Branch. In particular, grid stretching and refinement methods will be included in his study.

Research Summary Submitted by Fellow:

Detection of Directions of Gravity by Organisms and Contributions to Smaggice

I divided my time equally between two Glenn organizations and feel both interactions were beneficial. In the Microgravity Environment and Telescience Branch, I extended a study begun last year and produced a rough draft of a paper that will be revised and submitted for publication within a professional journal. My study focused upon a flagellated alga or other swimming microbe and the effect of gravity upon its swimming direction. It has long been known that many organisms tend to swim up or down on Earth. How organisms detect the direction of gravity is a question not fully resolved. The response of such organisms to reduced gravity or the absence of gravity is also of interest, particularly because the expected modified behavior may affect the health of astronauts.

Our theoretical model supposes the swimming organism is shaped like a spheroid. Its center of gravity is displaced a short distance from the geometric center, which coincides with the center of buoyancy, along the symmetry axis. In the absence of other orientating forces or torques, the action of gravity upon the organism tends to cause the embedded gravitational dipole to become vertically oriented. If the swimming force is directed along the symmetry axis, the organism will tend to swim up or down.

We supposed, however, that the organism is located within a fluid that is rotating slowly about a non-horizontal axis. If the rate of rotation is sufficiently slow and the organism is located sufficiently close to the axis of rotation, inertia of both fluid and organism may be neglected. Fluid rotation then gives rise to a hydrodynamic torque upon the organism that modifies its swimming direction (orientation). Despite the fluid rotation, the organism tends to achieve a stable, steady orientation. The mathematical model relates the swimming direction to the distance between the centers of mass and of buoyancy of the organism. If the swimming direction can be measured, one would have an estimate of this important distance for a given organism.

In principle, the orientation (and hence swimming direction) of an organism can be determined directly from microscopic observation. Alternatively, the swimming direction can be determined indirectly from the organism's trajectory within the rotating fluid. If the swimming force is constant, the organism will execute a helical trajectory. The axis of this trajectory and the axis of fluid rotation are parallel to each other, but the two axes are displaced from each other. This displacement is related to the swimming direction. Even if the swimming force is not constant, the swimming direction can still be determined from an appropriate integration of the organism's trajectory.

I also worked within the Icing Research Team. A significant activity of this branch, apart from operating the Icing Research Tunnel, is the development of computer codes that predict ice growth on airfoils and the effects of ice on aerodynamic performance. I contributed to the development of a future version of *SmaggIce*, which according to official sources is "a software toolkit used in the process of aerodynamic performance prediction of iced airfoils with ... Computational Fluid Dynamics (CFD). It includes tools for data probing, boundary smoothing, domain decomposition, and structured grid generation and refinement. SmaggIce provides the underlying computations to perform these functions, a GUI (Graphical User Interface) to control and interact with those functions, and graphical displays of results." The ultimate goal of *SmaggIce* and other efforts within the Icing Branch is to improve aviation safety.

My particular contributions to *SmaggIce* included the development of computer subroutines that enable grid redistribution and grid insertion. I also developed a code that predicts the location of the trailing edge point of a cut-off air foil. In grid redistribution, the user can specify the number of new grid points desired as well as the first and final grid spacings along a specified planar curve. New points are then distributed according to a hyperbolic tangent distribution. In grid insertion, the user specifies the number of new grid points to insert between existing grid points along a planar curve; these are uniformly distributed within each grid spacing. These two tools can be used in both directions of a 2D numerical grid, thereby leading to grid refinement. In the trailing edge problem, the trailing edge of airfoils within the Icing Research Tunnel is frequently cut-off for reasons of structural integrity; this airfoil modification does not affect lift or drag. But the cut-off airfoil presents difficulties in numerical simulations by inducing an unsteady mixing flow in the region. My subroutine predicts where the final trailing edge should be located.

Name: **Malik E. Elbuluk**
Education: Ph.D., Electrical Engineering
Massachusetts Institute of Technology

Permanent Position: Professor, Electrical Engineering
The University of Akron

Host Organization: Power and On-Board Propulsion Technology Division
Colleague: 5480/Richard L. Patterson

Assignment:

Development of Ultra-Low Temperature Motor Controllers

Professor Elbuluk will develop motor controller technology that will operate at ultra-low temperatures down to 35 K. This type of technology will be especially useful for motor systems located in ultra-low temperature environments such as those that are behind sun shields for deep space infrared telescopes. For such telescopes, stepper motors will be sued to position optical filter-wheels between the telescope optics and the sensing electronics. This will be groundbreaking work since motor controllers have never operated in such low temperature environments.

Research Summary Submitted by Fellow:

Ultra Low Temperatures Evaluation and Characterization of Semiconductor Technologies For The Next Generation Space Telescope

SUMMARY

I. Background

Electrical power components and systems in many future space missions, such as outer planetary exploration and deep space probes, must operate reliably and efficiently in very low temperature environments. Presently, spacecraft operating in the cold environment of deep space carry on-board a large number of radioisotope heating units to maintain an operating temperature for the electronics of approximately 25 °C. This is not an ideal solution because the radioisotope heating units are always producing heat, even when the spacecraft is already too hot, thus requiring an active thermal control system for the spacecraft. In addition, they are very expensive and require elaborate containment structures. Electronics capable of operation at cryogenic temperatures will not only tolerate the hostile environment of deep space but will also reduce system size and weight by eliminating radioisotope heating units and associated structures; thereby reducing system development and launch costs, improving reliability and lifetime, and increasing energy densities.

II. Ultra-Low Temperature Electronics Program at NASA Glenn Research Center

Electronics designed for low temperature operation will result in more efficient systems than room temperature. This improvement is a result of better electronic, electrical, and thermal properties of materials at low temperatures. In particular, the performance of certain semiconductor devices improves with decreasing temperature down to ultra-low temperature (-273 °C). The Low Temperature Electronics Program at the NASA Glenn Research Center focuses on research and development of electrical components and systems suitable for applications in deep space missions. Research is being conducted on devices and systems for use down to liquid helium temperatures (-273 °C). Some of the components that are being characterized include semiconductor switching devices, resistors, magnetics, and capacitors. The work performed this summer has focused on the evaluation of silicon-, silicon-germanium- and gallium-Arsenide-based (GaAs) bipolar, MOS and CMOS discrete components and integrated circuits (ICs), from room temperature (23 °C) down to ultra low temperatures (-263 °C).

III. Test Setup and Results

Power electronic circuits and ICs that can operate at cryogenic temperatures are crucial for space missions where ultra low temperatures are encountered. In particular, DC/DC and DC/AC converters supply power and provide control to motor loads and other peripheral loads.

The performance of off-the-shelf discrete electronic devices and integrated circuits (ICs) were evaluated at ultra low temperatures. The devices and ICs were selected have potential use in motor control systems for the Next Generation Space Telescope (NGST). The design of circuits and ICs included both bipolar- and CMOS-based technologies, using Silicon, Germanium, Silicon-Germanium and Galium-Arsenide semiconductor materials.

The tests were performed as a function of temperature using an environmental chamber utilizing liquid nitrogen as the coolant for temperature range 25 °C to –196 °C, and a chamber using liquid helium in the range 25 °C to –263 °C. At every test temperature, the devices and ICs under test were allowed to soak at that temperature for a period of 30 minutes before any measurements were made. After the last measurement was taken at the lowest temperature, the devices were allowed to stabilize to room temperature and then the measurements were repeated at room temperature to determine the effect of thermal cycling.

The test results showed that Silicon MOS- and CMOS-based devices and ICs perform well down to -263 °C whereas the Silicon bipolar-based devices ceased to operate at temperatures above liquid nitrogen (-196 °C). However, silicon-germanium and GaAs bipolar-based devices operated down to –263 °C.

Name: **Aryeh A. Frimer**
Education: Ph.D., Chemistry
Harvard University

Permanent Position: Professor, Chemistry
Bar Ilan University

Host Organization: Materials Division
Colleague: 5160/Mary Ann Meador

Assignment:

Norbornenyl end capped polyimides are widely used as polymer matrix composite materials for aircraft engine applications, since they combine ease of processing with good oxidative stability up to 300 °C. PMR resins are prepared via a two-step approach involving the initial formation of oligomeric pre-polymers capped at both ends by a reactive end cap. The end cap undergoes crosslinking during processing, producing the desired low density, high specific strength materials. It is the end cap that facilitates processing by controlling molecular weight of the oligomer and allowing flow before crosslinking. However, it is this very end cap that accounts for much of the weight loss in the polymer on aging in air at elevated temperatures. Designing new end caps to slow down degradation has the potential to substantially prolong the lifetime of the material.

Previously, we reported studies on ^{13}C labeled PMR-15 in which we followed the thermo-oxidative aging of end cap by solid NMR. Based on the study, two major pathways of end cap degradation were identified. One path leads to much weight loss in the polymer. The other leads to more stable structures that form a protective layer on the surface. We are working toward the design of new end caps that favor the latter type of degradation. Several different structures are currently under investigation.

Research Summary Submitted by Fellow:

New Endcaps for Improved Oxidation Resistance in PMR Polyimides

A polyimide is a polymer composed of alternating units of diamine and dianhydride, linked to each other via an imide bond. PMR polyimides, commonly used in the aerospace industry, are generally capped at each end by an endcap (such as the nadic endcap used in PMR 15) which serves a double function: (1) it limits the number of repeating units and, hence, the average molecular weight of the various polymer chains (oligomers), thereby improving processibility; (2) Upon further treatment (curing), the endcap crosslinks the various oligomer strands into a tough heat-resistant piece. It is this very endcap, so important to processing, that accounts for much of the weight loss in the polymer on aging in air at elevated temperatures. Understanding this degradation provides clues for designing new endcaps to slow down degradation, and prolong the lifetime of the material.

We have previously reported[i,ii] studies on the thermo-oxidative aging of a modified PMR-15, in which we labeled the endcap at the methyne carbon □to the carbonyl groups with ^{13}C (shown in the Scheme 1 below labeled with a star).

Scheme 1: PMR Degradation Pathways

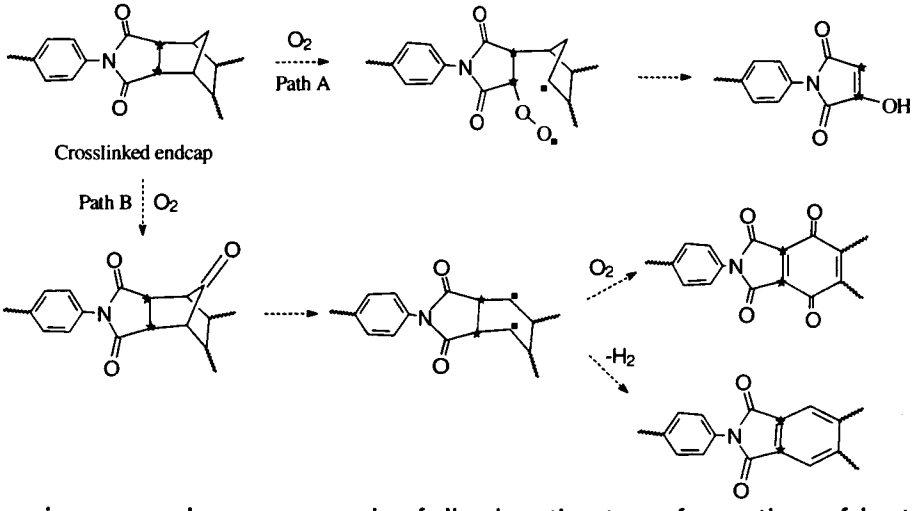

Though aging is a complex process, by following the transformation of just this carbon by solid NMR, we have been able to identify two major degradation pathways for endcap oxidation. Path A produces cleavage products which lead to large weight losses, while path B forms stable oxidation products with much smaller associated weight losses. These stable products also help to form a surface layer on the polymer which protects the interior from further oxidation.

We have embarked on the synthesis of replacement endcaps that favor path B and lead to lower weight loss and, hence, less shrinkage and cracking in the oxidation layer.[iii] We have proposed to utilize structures like **1** below. Our theory is that using an X group more labile than the methylene in the parent norbornenyl-end cap could actually improve oxidative stability. Over the past three summers, we have explored the effect of replacing the nadic end-cap of PMR-15 with the 7-hydroxy analog of nadic anhydride (X=CH-OH).[iv]

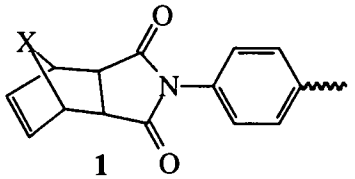

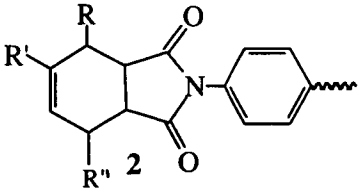

X=CO, CO_2, O, CHOH, CF_2
R= H, Ph, OCH_3, or $OSiCH_3$
R'=H, CH_3
R"=Ph

However, we must also consider 1,2,3,6-tetrahydrophthalimide **2** as an end cap that contains no X group at all. This structure was investigated by TRW and at NASA in the 1980's and found to yield composites with TOS values better than PMR-15, but quite frangible.[v] St. Clair and St. Clair[vi] as an end cap for polyimide adhesives. However, they found no evidence of cross-linking in this system until 415 °C. If the cross-linking temperature could be lowered—either by substitution on the ring or by catalysis—this might be a viable replacement for the norbornene end cap. Indeed, onset of decomposition for polymers made with this end cap was shown to be at a higher temperature than for the norbornenyl-end cap.

We have synthesized several substituted tetrahydrophthalic anhydride endcaps, including the 3-hydro, 3-phenyl, 3-methoxy, 3-trimethylsilyloxy, 4-methyl and 3,6-diphenyl analogs via the Diels-Alder condensation of the corresponding butadienes[vii] and maleic anhydride. The anhydrides were then reacted with methylenedianiline generating imides **6**.

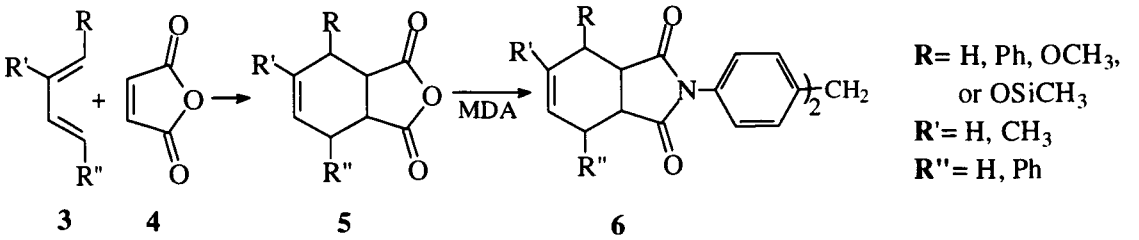

3 **4** **5** **6**

These PMR model compounds (n=0) were heated gradually to 370 °C (700 °F) and the thermal-oxidative transformations followed by NMR. Analysis of the data indicates that the tetrahydrophthalic endcaps undergo not only cross-linking, but aromatization as well. It is this substantial percentage of aromatic product that is responsible for both the observed improved TOS tetrahydrophthalic endcapped polyimides and their substantial frangibility.

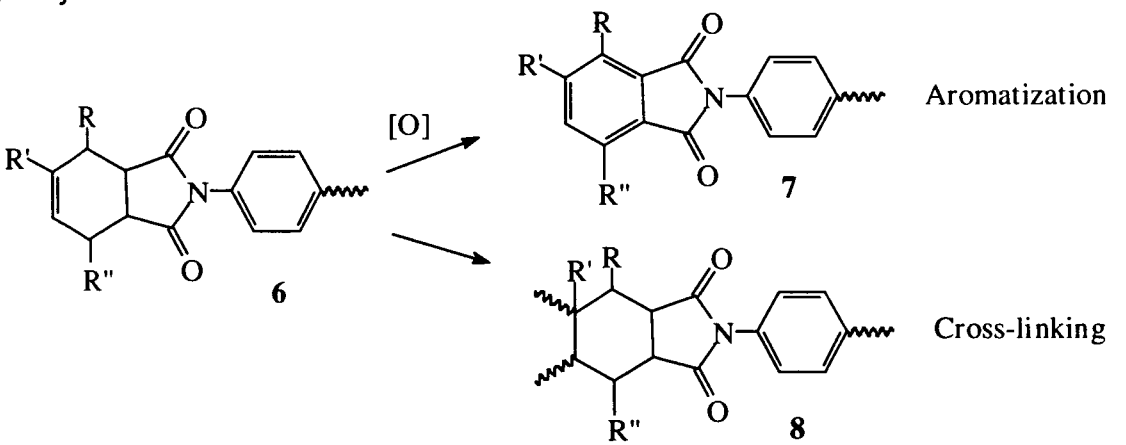

When the thermolysis is carried out under nitrogen (in an isothermal TGA) aromatization was largely inhibited. We are presently investigating the results of processing tetrahydrophthalic endcapped polyimides under inert atmosphere.

References and Notes

1. Meador, M. A. B.; Johnston, J. C.; Cavano, P. J.; Frimer, A. A. *Macromolecules* **1997**, *30*, 3215-3223.
2. Meador, M. A. B.; Johnston, J. C.; Frimer, A. A.; Gilinsky-Sharon, P. *Macromolecules* **1999**, *32*, 5532-5538.
3. Meador, M. A. B.; Lowell, C. E.; Cavano, P. J.; Herrera-Fierro, P. *High Perform. Polym.* **1996**, *8*, 363-379.
4. (a) Meador, M. A. B.; Johnston, J. C.; Hardy-Green, D.; Frimer, A. A.; Gilinsky-Sharon, P.; Gottlieb, H.E. *Chemistry of Materials,* **13**, 2649-2655 (2001); (b) Meador, M. A. B.; Frimer, A. A. "End Caps Increase Thermo-Oxidative Stability of Polyimides," *NASA Tech Briefs*, October 2001, LEW-16987. This paper was awarded a NASA Certificate of Recognition for Technical Innovation. (c) Meador,

M. A. B.; Frimer, A. A. "Polyimides and Process for Preparing Polyimides Having Improved Thermal-Oxidative Stability," U.S. Patent Number 6,303,744, October 16, 2001.

5. Alston, W.B. personal communication (August 2002) regarding unpublished results.
6. St. Clair, A. K.; St. Clair, T. L. *Polym. Eng. Sci.* **1982** *22*, 9-14.
7. The butadienes are commercially available, with the exception of *trans*-1-phenylbutadiene: Grummit, O.; Becker, E.I. *Org. Synthesis*, Coll. Vol. **IV**, 771 (1963).

Name: **Vladimir V. Golubev**
Education: Ph.D., Aerospace Engineering
University of Notre Dame

Permanent Position: Assistant Professor, Aerospace Engineering
Embry-Riddle Aeronautical University

Host Organization: Structures and Acoustics Division
Colleague: 5940/James R. Scott

Assignment:

Very Large Eddy Simulation Technique for Noise Prediction and Control in Turbomachinery and Propulsion

Implement a low-order, implicit A-stable time-stepping scheme in the CAA code of Dr. Ray Hixon. Apply the resulting Very Large Eddy Simulation (VLES) code to the problem of viscous gust-airfoil interaction. Investigate the accuracy of different turbulence models. As time permits, validate the VLES code on various test cases, including a supersonic jet and swirling flow downstream of a rotor stage.

Research Summary Submitted by Fellow:

Very Large Eddy Simulation Technique for Noise Prediction and Control in Turbomachinery and Propulsion

The summer fellowship research project focused on further developing an advanced computational technique based on Very Large Eddy Simulation (VLES) for analysis and control of major sources of noise in turbomachinery and propulsion systems, including jet noise and fan noise. Major part of the work during the 10-week tenure dealt with implementing a low-order, implicit A-stable time-stepping scheme in the existing explicit VLES code of Dr. Ray Hixon. The preliminary plan of the work also included application of a new time marching formulation to the problem of viscous gust-airfoil interaction. Other research items selected for implementation (possibly in the future) included investigating a set of new subgrid turbulent models for the code, and code application to a number of test cases, including a supersonic jet and swirling flow downstream of a rotor stage.

The following items were addressed during the 10-week tenure:

- **Implicit Time Marching**

  The original version of the VLES code uses a sixth-order prefactored compact scheme for spatial discretization, and an optimized, *explicit* fourth-order Runge-Kutta scheme (RK56) for time stepping. The high-accuracy explicit time stepping method has been used to ensure the accurate propagation of waves through even the smallest grid cells. While this may be appropriate for inviscid-flow grids, where the

range of grid cell sizes is small, it is not good for highly-clustered viscous-flow grids due to the excessively small time step required for stability. The current study examined several alternatives for implementing time-accurate implicit marching in the code. To become an effective tool, the iterative procedure implemented at each time step of the implicit time marching must converge quickly, with minimal numerical overhead. In order to prove the value on the implicit marching concept for the VLES code, a low-order accurate scheme was implemented with simple corrector-type functional subiterations that are computationally efficient for non-stiff problems. In addition, a number of methods to accelerate subiteration convergence were examined for possible future implementation, including Runge-Kutta subiterations, preconditioning using a low-order explicit stencil combined with line relaxation, Alternating Direction Implicit (ADI) method, multigrid method, and a Generalized Minimal Residual (GMRES) method. Higher-order implicit marching schemes were reviewed, including recently developed, promising algorithms based on *(i)* the second-order implicit/explicit marching; *(ii)* a non-oscillatory implicit scheme with time limiters removing severe time step restrictions typical of high-order implicit schemes with time linearity; and *(iii)* Additive Semi-Implicit Runge-Kutta (ASIRK) methods which allow to treat stiff terms implicitly and non-stiff terms explicitly. In the future research, the benefits of low-order and high-order schemes will be compared, as indicated below.

While possible benefits of different implicit and semi-implicit schemes were investigated for future application, the proof-of-concept work focused on implementing the first- order backward Euler scheme and fitting the implicit time marching procedure in the general structure of the VLES code. The results of numerical tests were examined for two cases: *(i)* a Gaussian low-amplitude density pulse in a 2D domain with Cartesian grid and periodic boundary conditions, and *(ii)* a 2D flow around loaded airfoil in a domain with curvilinear grid and inflow/outflow radiation boundary conditions. The results shown below indicate that the implicit time marching scheme with functional subiterations is producing stable convergence, which in general is a function of selected numerical parameters including relaxation factor and criterion on residual convergence. In Figure 1, the calculated contour plots for propagation of the Gaussian density pulse are compared between the currently used explicit RK56 method (with CFL number equal to 1) in Figure 1a, and the new implicit (IMP) formulation with CFL numbers 0.1, 1, 2, and 4 (In Figures 1b-e, respectively). Stability range for the increasing CFL number was examined to test the future ability of the VLES code to produce overall time-accurate calculations with high grid clustering in the boundary layers (e.g., over an airfoil or a jet nozzle duct). Note that even though the solution remains stable for the shown range of CFL numbers, the first-order backward Euler scheme is producing (as expected) high dissipation and moderate dispersion, clearly seen from the 2D comparison obtained from the domain cut at y=0.5 and shown in Figure 2. It may be concluded that for time-accurate solutions of unsteady problems, a trade-off between the low-order and high-order implicit schemes should be investigated based on the required accuracy of resolution for the selected frequency band, and the computational cost. Note that for a steady-state solution (obtained, e.g., for the flow around a loaded airfoil), a low-order scheme may be adequate since the accuracy of time marching is not an issue. For acoustic radiation resulting from the viscous gust-airfoil interaction, the CFL

number may be based on the accuracy required for the inviscid region, while the refined mesh in the viscous region may have very high CFL numbers just to ensure stability. Immediate extension of this work will include investigation and implementation of acceleration algorithm for subiteration convergence, and subsequent investigation of the higher-order schemes.

- **Non-Reflecting Boundary Conditions for High-Frequency Calculations**

  An issue of proper outflow boundary conditions for nonlinear VLES study of gust-airfoil interaction was investigated. The current formulation based on the standard radiation condition and Tam-Webb condition led to unstable solutions for reduced gust frequencies above one, which was attributed to spurious reflections building up in the computational domain due to the fact that the radiation conditions employ the linear theory and a point source assumption. Future work will focus on resolving this issue to extend the low-frequency nonlinear analysis to higher frequencies, more typical of unsteady rotor-stator interactions. A collaboration was started with Prof. Thomas Hagstrom who proposed to use his formulation of the boundary conditions based on the Perfectly Matched Layer (PML) approach solving an auxiliary set of equations in the far-field absorption layer. A code employing these conditions for the LEE solver with two periodic boundaries was made available and tested for proper absorption of the radiated sound. Results indicate a proper decay of a single-pulse solution throughout the computational domain, with some residual low-amplitude standing waves localized in the absorption layer. Extension to the high-frequency, nonlinear gust-airfoil interaction problem will involve careful treatment of corners of the computational domain in the case without a periodic boundary interface.

- **NASA Presentation**

  Results of the ongoing research and collaboration with NASA colleagues were reported in two presentations given for the NASA Glenn Structures and Acoustics Division (also prepared for the 8th AIAA/CEAS Aeroacoustics Conference): *(i)* "Nonlinear Analysis of Airfoil High-Intensity Gust Response Using a High-Order Prefactored Compact Code", and *(ii)* "Prediction of the Acoustic Field Associated with Instability Wave Source Model for a Compressible Jet".

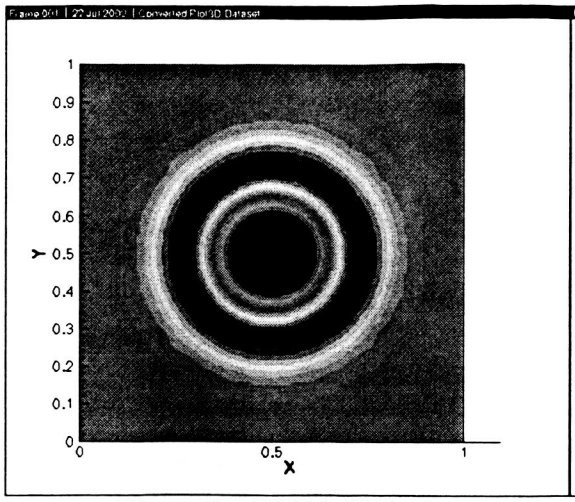

Figure 1a: RK56, CFL=1

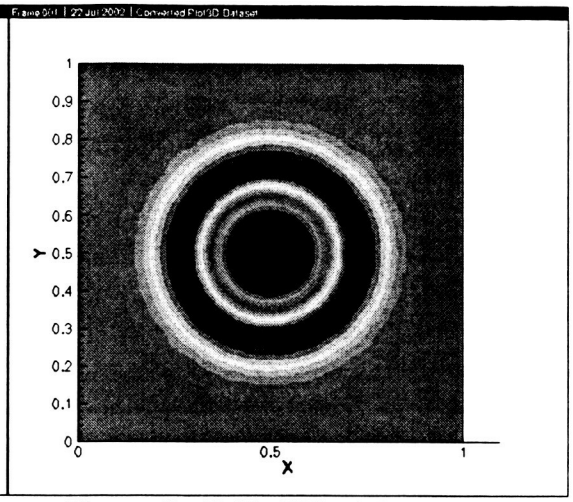

Figure 1b: IMP, CFL=0.1

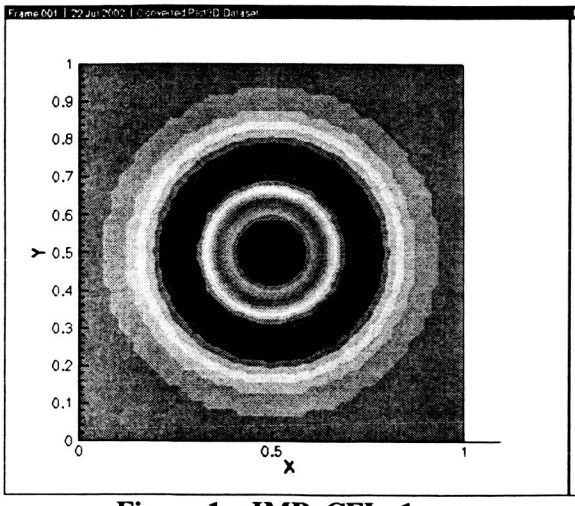

Figure 1c: IMP, CFL=1

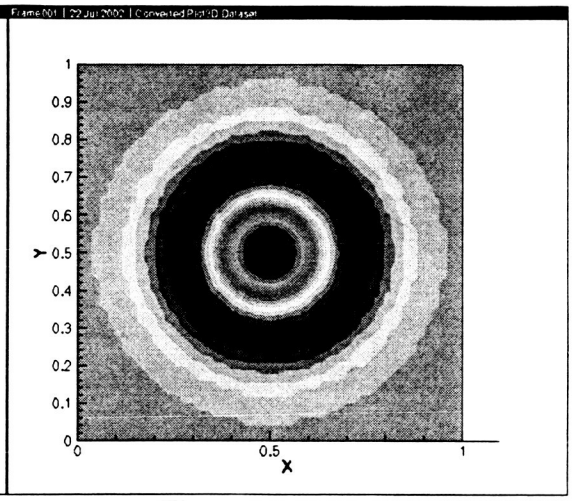

Figure 1d: IMP, CFL=2

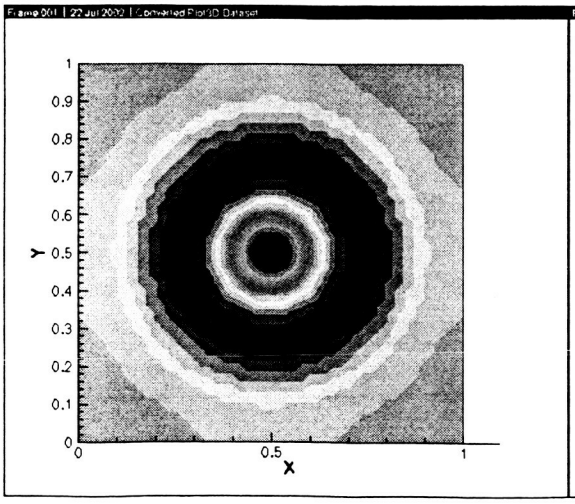

Figure 1e: IMP, CFL=4

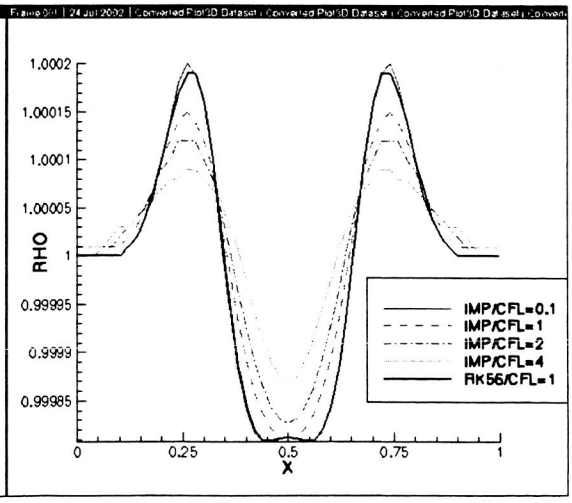

Figure 2: Comparison, cut at y=0.5

Name: **Osama M. Jadaan**
Education: Ph.D., Engineering Mechanics
Penn State University

Permanent Position: Professor, General Engineering
University of Wisconsin-Platteville

Host Organization: Structures and Acoustics Division
Colleague: 5920/Noel N. Nemeth

Assignment:

Development of Probabilistic Life Prediction Methodologies and Testing Strategies for MEMS

This effort is to investigate probabilistic life prediction methodologies for MicroElectroMechanical Systems (MEMS) and to analyze designs that determine stochastic properties of MEMS. This includes completion of a literature survey regarding Weibull size effect in MEMS and strength testing techniques. Also of interest is the design of a proper test for the Weibull size effect in tensile specimens. The Weibull size effect is a consequence of a stochastic strength response predicted from the Weibull distribution. Confirming that MEMS strength is controlled by the Weibull distribution will enable the development of a probabilistic design methodology for MEMS - similar to the GRC developed CARES/Life program for bulk ceramics. Another potential item of interest is analysis and modeling of material interfaces for strength as well as developing a strategy to handle stress singularities at sharp corners, filets, and material interfaces. The ultimate objective of this effort is to further develop and verify the ability of the Ceramics Analysis and Reliability Evaluation of Structures/Life (CARES/Life) code to predict the time-dependent reliability of MEMS structures subjected to multiple transient loads. Along these lines work may also be performed on transient fatigue life prediction methodologies.

Research Summary Submitted by Fellow:

Probabilistic Life Prediction and Testing Strategies for MEMS

My activities this summer focused on three efforts:

1. My first effort finalized the work started last summer. The objective of that work was to review the MEMS literature for evidence of probabilistic behavior in the mechanical properties of MEMS (especially strength), and to investigate whether evidence exists that a probabilistic Weibull effect exists at the structural microscale. Since many MEMS devices are fabricated from brittle materials, then that raises the question whether these miniature structures behave similar to bulk ceramics. For bulk ceramics, the term Weibull effect is used to indicate that significant scatter in fracture strength exists, hence requiring probabilistic rather than deterministic treatment. In addition, the material's strength behavior can be described in terms of the Weakest Link Theory (WLT) leading to strength dependence on the component's

size (average strength decreases as size increases), and geometry/loading configuration (stress distribution). Test methods used to assess the mechanical properties of MEMS, especially strength, were reviewed. Four materials commonly used to fabricate MEMS devices were reviewed. These materials are polysilicon (most widely used material in MEMS fabrication), single crystal silicon (SCS), silicon nitride, and silicon carbide. The results of this study, titled "Probabilistic Weibull Behavior and Mechanical Properties in Brittle MEMS Devices," were submitted and accepted for publication as a book chapter to be published next year. The book will be titled *Mechanical Properties of MEMS Structures.*

2. My second effort this summer dealt with designing MEMS test specimens to be used for predicting the structural and probabilistic behavior of SiC MEMS devices utilized in harsh environments. This work was requested as part of the Advanced Micromachining Technology for SiC Microengine project. This project is part of the Revolutionary Aeropropulsion Concepts (RAC) program. A report was submitted to both the Sensors & Electronics Branch, 5510, and the Life Prediction Branch, 5920.

   Mechanical design of MEMS requires the ability to predict the strength of load-carrying components with stress concentrations. The majority of these microdevices are made of brittle materials such as polysilicon, which exhibit higher fracture strengths when smaller volumes or areas are involved. A review of the literature shows that the fracture strength of polysilicon increases as tensile specimens get smaller. Very limited results show that fracture stresses in brittle MEMS structures with stress concentrations are larger than what would be predicted based on stress concentration factor analysis. This is because of the decreased size of highly stressed regions. This is an important consideration in the design of MEMS fabricated from brittle materials. One usually thinks of stress concentrations as weak points in a mechanical structure, and indeed the stress is highest there. However, structures can sustain higher fracture stresses because the volume or area of highly stressed regions is smaller. One must obviously know the variation of the strength with size to benefit from this considerable advantage.

   Microtensile specimens displaying intermediate effective sizes between straight and edge-notched coupons were designed in order to have at least three evenly spaced data sets on a fracture strength vs. effective size (volume or area) plot. Two tensile specimens, circular edge and elliptic edge, were designed and analyzed. After preliminary analysis only the circular edge specimen was fully studied and ultimately recommended. FEA analysis and probabilistic CARES/Life (Ceramic Analysis and Reliability Evaluations of Structures Life Prediction) code effective size calculations results for all four specimens (straight, notched, circular edge and elliptic edge) were tabulated and plotted as function of the Weibull modulus, m. Effective sizes and predicted strengths were calculated for Weibull moduli varying between 5 and 25, since it is not known what will be the actual m for the SiC microtensile specimens when they are tested. A specific specimen geometry was recommended for the test program that would optimize the prediction methodology of the integrity of MEMS structures.

3. Present capabilities of the NASA CARES/Life code include probabilistic life prediction of ceramic components subjected to fast fracture, slow crack growth (SCG), and fatigue failure modes. Currently, this code has the capability to compute the time-dependent reliability of ceramic structures subjected to simple time-dependent loading. For example, in SCG type failure conditions CARES/Life can handle the cases of sustained and linearly increasing time-dependent loads, while for cyclic fatigue applications various types of repetitive constant amplitude loads can be accounted for. In real applications applied loads are rarely that simple, but rather vary with time (start up, shut down, dynamic, and vibrational loads). In addition, when a given component is subjected to transient environmental conditions and or thermal loading, the material properties also vary with time. This adds another degree of complexity to the problem at hand. Recently, a transient probabilistic capability was added to the CARES/Life code. Therefore, my third activity this summer was to verify the fidelity of this capability by applying it to predict the reliability a thermally shocked SiC tubes. These tubes were heated to 1000 °C and thermally quenched down by blasting their external surfaces with air. The transient heat transfer and the resulting time-dependent theromealstic multiaxial stresses were modeled using the ANSYS Finite Element Analysis code. Subsequently, CARES/Life was used to compute the reliability at the end of the five cycles, 10-second per cycle quench period. Experimental data indicated that 55% of the SiC tubes failed at the end of five cycles, while the analysis predicted that 90% of the tubes would fail. It is to be emphasized that the thermoelastic FEA analysis, which involved reverse heat transfer analysis to get as close as possible to measured temperatures at the internal surfaces of tubes, was exceedingly difficult. A 10% decrease in the computed stresses would yield a predicted failure probability of 55% that matches the experimental data.

Name: **Ivana M. Milanovic**
Education: Ph.D., Mechanical Engineering
Polytechnic University

Permanent Position: Assistant Professor, Mechanical Engineering Technology
University of Hartford

Host Organization: Turbomachinery and Propulsion Systems Division
Colleague: 5860/Khairul B. Zaman

Assignment:

During her visit last summer, Professor Milanovic conducted wind tunnel experiments on jets in cross flow. In her anticipated visit during the upcoming summer, she plans to continue on the same project investigating further aspects of the problem. This will involve mainly hot-wire anemometer measurements in the low-speed wind tunnel with 'pitched' and 'yawed' jets discharging into the cross-flow of the wind tunnel. She will also participate in experiments involving 'synthetic jets' in cross-flow. This will involve jets produced by periodic excitation by a loudspeaker without involving any air supply for the jet. The overall goal will be to obtain database and investigate flow control strategies. The research will be of fundamental nature. The wind tunnel facilities are located in the Test Cells CW13 and CW15 of the Engine Research Building. As the NASA Colleague, I will be directly collaborating with Professor Milanovic in these experiments. Depending on the progress of the experiment, she would also like to initiate numerical simulation of the subject flow with collaboration from other colleagues of the Nozzle Branch.

Research Summary Submitted by Fellow:

Synthetic Jets

An experimental investigation on isolated and clustered synthetic jets with and without cross-flow has been conducted in the NASA GRC subsonic wind tunnel. Recent development for jets in cross-flow (JICF) flowfield involves introducing pulsating jet into the flow, instead of a steady high momentum jet. The pulsating jet can be generated by a cavity-membrane configuration attached to the jet orifice, and this scheme is commonly called a "synthetic jet", as no actual pneumonic device has been used to generate the jet. The basic idea of a synthetic jet (SJ) is as follows: a forward motion of the actuator diaphragm results in the ejection of fluid from the jet cavity and leads to the formation of the vortex ring. The vibrating cycle continues so that a train of rings is generated to form a high momentum jet into the flow. It has been shown that the vortical structure continues its roll up with the downstream advection until small-scale disturbances of the core result in the transition to turbulence and a reduction in advection velocity.

The current study was conducted in a NASA GRC open circuit low-speed wind tunnel with 0.76 m x 0.51 m test section. The tunnel has a free stream turbulence level of 0.1%. Synthetic jets originating from orifices of different geometry and sizes were

created by a loudspeaker housed in a chamber underneath the tunnel test section as seen in Fig. 1. Helmhotz resonance of the chamber is utilized to produce the highest sound pressure level for the given cavity volume of 1700 in^3. The amplitude of the membrane was controlled by varying the amplitude of the sinusoidal driving signal. Forcing frequencies were between 12.5 Hz and 118 Hz, whereas the amplitudes of the driving signal spanned the range from 0.67 V to 9.6 V. The jets exited orifices of cylindrical tapered and slanted shape, all of which had 0.75" diameter. Additionally, cylindrical orifice diameter was also set at 0.375, 1.5 and 3", and the cluster of cylindrical orifices was examined for the diameter 0.25". The orifices were straight holes cut through a clear plastic disc of 25.4 mm thickness. The disc was mounted flush on the test section floor. Orifice pitch, measured between the nozzle centerline and the flow of the test section was set at $\alpha = 20^0$. Disk could be rotated to vary the yaw angle, β, measured between the nozzle centerline and the direction of the cross flow. The jet was yawed to 45^0. In the case of synthetic jets in the cross flow (SJCF) all data were acquired for a constant free stream velocity of $U_\infty = 20$ ft/s.

The measurements were performed by hot-wire anemometry using a single hot wire and two ×-wires of different orientations. Single hot-wire was centered spanwise and traversed in the vertical and cross-flow directions thereby obtaining centerline velocity profiles and 'SJ trajectory'. Two ×-wires were used for flow mapping in the cross-flow plane. Probes were traversed under automated computer control. The ×-wire pair was stepped through the same grid points allowing the measurement of all three components of mean velocity and turbulence intensity. Hot-wire signal indicated flow reversal in the streamwise region extending up to half a diameter away from the orifice. The origin of the coordinate system is located at the center of the jet orifice. The streamwise (i.e., the cross-flow) direction is denoted by *x*, the direction normal to the tunnel floor is denoted by *y*, and the spanwise direction along the tunnel floor by *z*. Measurements of SJCF were taken at the downstream locations of 0.5, 5 and 10 jet diameters from the orifice. Detailed hotwire anemometry surveys provided mean velocity (*u, v, w*) and turbulence intensity (*u', v', w'*) data from which vorticity distribution (ω_x, ω_y, ω_z), as well as contours of $\overline{u'v'}$ and $\overline{u'w'}$ could be inferred. All quantities were normalized by the freestream velocity, U_∞, and the jet diameter, *D*.

Synthetic jet has a zero mean flow rate at the exit plane, and in order to characterize various synthetic jets and eventually compare them with continuous jets, the characteristic velocity was calculated using Smith and Glazer[1] definition:

$$V_o = L_o f = f \int_0^{T/2} v_o(t)dt$$

where $v_o(t)$ is the streamwise velocity averaged over the orifice area, $T = 1/f$ is the oscillation period, and L_o or the stroke length is the length of the fluid slug ejected from the nozzle during the blowing stroke. Phase-averaged hot-wire output was measured at the orifice centerline, 0.2 diameters above the tunnel wall, furnishing characteristic velocities. Dimensionless stroke lengths L_0/D for different SJ configurations examined

[1] Smith, B. L., and Glezer, A., The formation and evolution of synthetic jets, *Phys. Fluids,* 10 (9): 2281-2297, 1998.

in the current work are listed in Table 1. Normalized centerline velocity profiles for SJ's without cross-flow and selected cases of Table 1 are presented in Fig.2. Clearly there is a limiting value of L_0/D at which the centerline velocity profile shows an initial peak and subsequently decays. Following the nomenclature of Gharib et al.[2] this value is referred to as the formation number, and its magnitude in the present study is found to be one.

Trajectories of SJCF for cylindrical and pitched orifices based on maximum values of fundamental (r.m.s.) intensity, u'_{fmax}, with accompanying predictions for steady JICF are shown in Fig. 3 for diameters of 0.75", f_p = 25 Hz, A = 9.6 V, and U_∞ = 20 ft/s. It appears that trajectory of synthetic jet from cylindrical orifice coincides with that of normal jet in a cross flow, as predicted by Zaman and Foss[3].

Detailed data in the cross-section plane have been acquired for all orifice geometries at locations of 0.5, 5 and 10 jet diameters downstream from the orifice. Streamwise mean velocity and vorticity contours as well as contours of turbulence intensity for SJCF from cylindrical orifice are shown in Figs. 4-6 at x/D = 5, z/D = 0, f_p = 25 Hz, A = 9.6 V, and U_∞ = 20 ft/s. It has been observed that the synthetic jet behaves similar to a steady jet in the cross-flow, and the SJ from the cluster of orifices is found to be comparable to the SJ from single orifice.

In summary, current investigation of synthetic jets and synthetic jets in cross-flow examined the effects of orifice geometry and dimensions, momentum-flux ratio, cluster of orifices, pitch and yaw angles as well as streamwise development of the flow field. This comprehensive study provided much needed experimental information related to the various control strategies. The results of the current investigation on isolated and clustered synthetic jets with and without cross-flow will be further analyzed and documented in detail. Presentations at national conferences and publication of peer-reviewed journal articles are also expected. Projected publications will present both the mean and turbulent properties of the flow field, comparisons made with the data available in an open literature, as well as recommendations for the future work.

The authors are thankful to Dr. Frank Montegani and Ms. Toni Rusnak for their organizational leadership.

[2] Gharib, M., Rambod, E., and Shariff, K., A universal time scale for vortex ring formation, *J. Fluid Mech.*, 360: 121-140, 1998.

[3] Zaman, K. B. M. Q., and Foss, J. K., The effect of vortex generators on a jet in a cross-flow, *Phys. Fluids,* 9 (1): 106 – 114, 1997.

Table 1 **Initial condition for different SJ Configurations.**

Case	D (in)	f_p (Hz)	A (Vrms)	V_0 (ft/s)	L_0/D
1	0.75	12.5	0.67	1.6	2.0
2	0.75	12.5	2.3	8.5	10.9
3	0.75	12.5	5.8	26.1	33.4
4	0.75	12.5	9.6	36.1	46.2
5	0.75	25	0.67	5.1	3.3
6	0.75	25	2.3	18.4	11.8
7	0.75	25	5.8	35.4	22.7
8	0.75	25	9.6	48.8	31.2
9	0.75	50	0.67	2.1	0.7
10	0.75	50	2.3	7.1	2.3
11	0.75	50	4.6	15.6	5.0
12	0.75	50	9.6	38.2	12.2
13	0.75	118	6.0	7.8	1.1
14	0.375	25	9.6	43.1	55.2
15	1.5	38	9.6	41.0	8.6
16	3.0	65	2.3	8.0	0.5
17	3.0	65	9.6	22.6	1.4

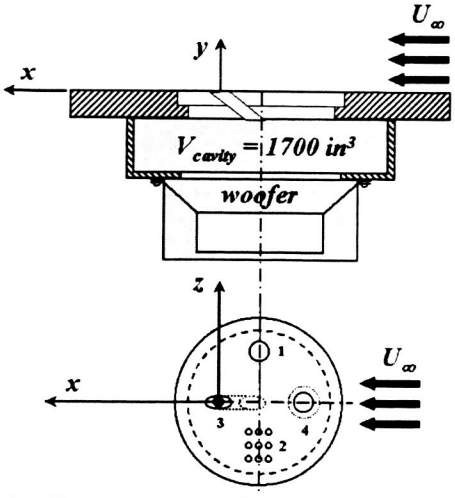

Fig. 1 Experimental Set Up. Orifice configurations:
(1) cylindrical, (2) clustered, (3) pitched, (4) tapered.

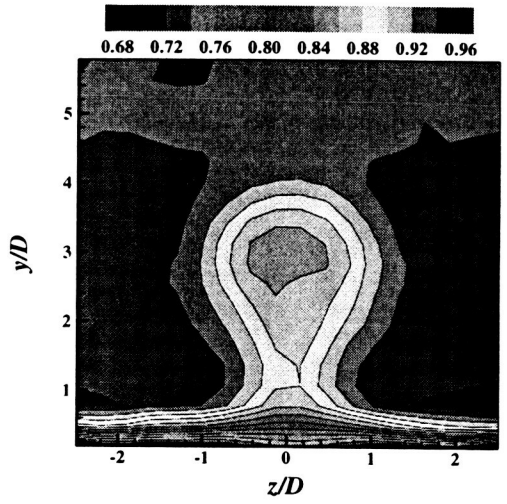

Fig. 4 Streamwise mean velocity contours for SJCF from cylindrical orifice; x/D = 5, z/D = 0, f_p = 25 Hz, A = 9.6 V, U_∞ = 20 ft/s.

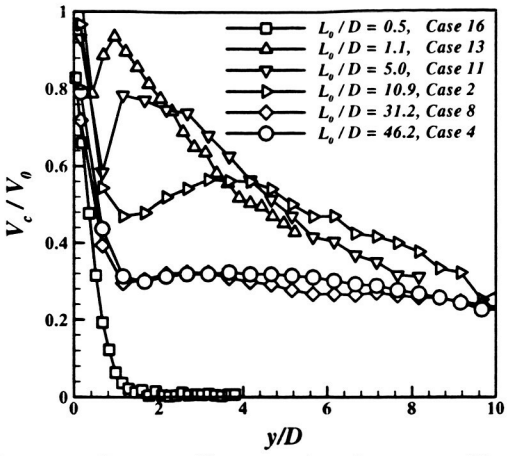

Fig. 2 Centerline velocity profiles for SJ's without cross-flow (U_∞ = 0); x/D = 0, z/D = 0. Cases refer to Table 1.

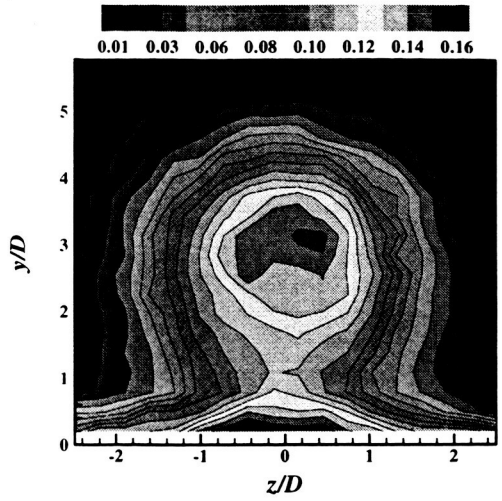

Fig. 5 Streamwise contours of turbulence intensity for SJCF from cylindrical orifice; x/D = 5, z/D = 0, f_p = 25 Hz, A = 9.6 V, U_∞ = 20 ft/s.

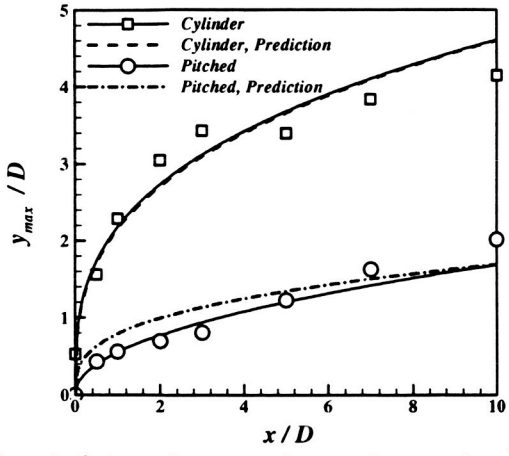

Fig. 3 SJ trajectory based on u'_{fmax} with accompanying theoretical prediction for D = 0.75" orifice; z/D = 0, f_p = 25 Hz, A = 9.6 V, U_∞ = 20 ft/s, (a) Cylindrical, (b) Pitched.

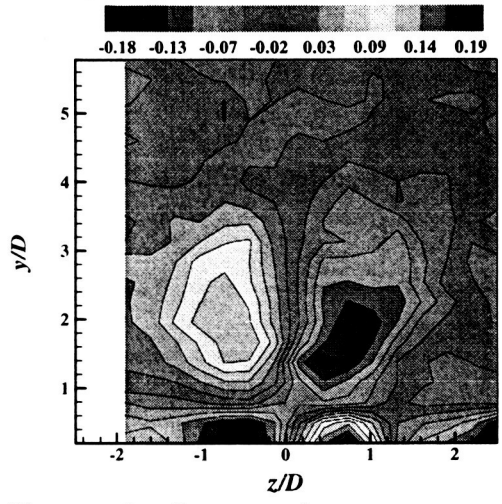

Fig. 6 Streamwise mean vorticity contours for SJCF from cylindrical orifice; x/D = 5 z/D = 0, f_p = 25 Hz, A = 9.6 V, U_∞ = 20 ft/s.

Name: **Dimitris E. Nikitopoulos**
Education: Ph.D., Mechanical Engineering
Brown University

Permanent Position: Associate Professor, Mechanical Engineering
Louisiana State University

Host Organization: Instrumentation and Controls Division
Colleague: 5530/Dennis E. Culley

Assignment:

Active Control of Jets in Cross-Flow for Film Cooling Applications

Jets in cross-flow have applications in film cooling of gas turbine vanes, blades and combustor liners. Their cooling effectiveness depends on the extent to which the cool jet-fluid adheres to the cooled component surface. Lift-off of the cooling jet flow or other mechanisms promoting mixing, cause loss of cooling effectiveness as they allow the hot "free-stream" fluid to come in contact with the component surface. The premise of this project is that cooling effectiveness can be improved by actively controlling (e.g. forcing, pulsing) the jet flow. Active control can be applied to prevent/delay lift-off and suppress mixing. Furthermore, an actively controlled film-cooling system coupled with appropriate sensory input (e.g. temperature or heat flux) can adapt to spatial and temporal variations of the hot-gas path. Thus, it is conceivable that the efficiency of film-cooling systems can be improved, resulting in coolant fluid economy. It is envisioned that Micro Electro-Mechanical Systems (MEMS) will play a role in the realization of such systems. As a first step, a feasibility study will be conducted to evaluate the concept, identify actuation and sensory elements and develop a control strategy. Part of this study will be the design of a proof-of-concept experiment and collection of necessary data.

Research Summary Submitted by Fellow:

Towards Active Control of Heat Transfer in the Hot Gas Path of Gas Turbines

The general objective of this summer project was to take the first steps towards the development of a program in the area of active control in the hot gas path of gas turbine engines. The project supports the development of intelligent engines (NASA-GRC Aeropropulsion - Gas Turbine Revolution) and has excellent potential to finding application in distributed vectored and hybrid propulsion systems (NASA-GRC Aeropropulsion goals). It is also directly relevant to Goal One/Objectives 1&2 of NASA's Aerospace Technology Enterprise Strategic Plan because it contributes to increasing safety and reducing emissions of gas-turbine propulsion systems. The specific objective of the project was to investigate the development and implementation feasibility of active control of the film-cooling process. This process is essential to the protection of hot-gas-path components (turbine vanes, blades, endwalls and combustor liners), the increase in specific thrust and reduction of specific fuel consumption of gas turbine engines.

The first part of the study was devoted to assessing the potential benefits of the development of an actively controlled film-cooling system. The results of this assessment are summarized in the figure below where both increases in performance and intangible ones are indicated.

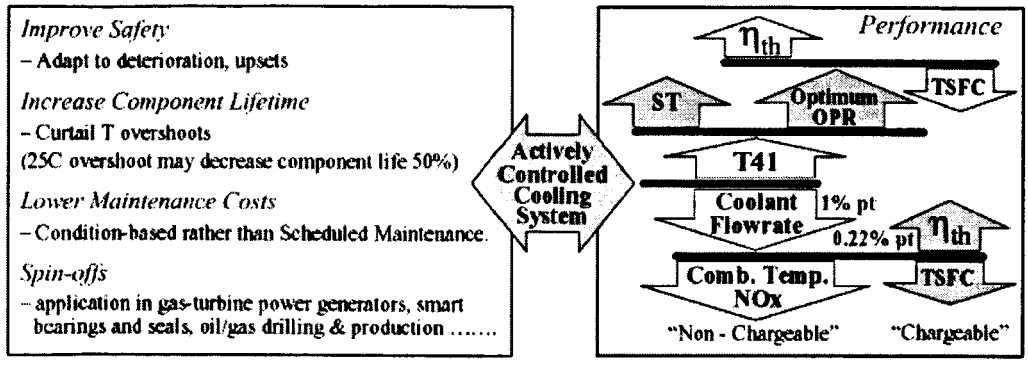

ST – Specific Thrust $T / \dot{m}_{air}$ OPR – Overall Pressure Ratio

η_{th} – Thermal Efficiency TSFC – Thrust Specific Fuel Consumption $\dot{m}_{fuel} / T$

The premise for this project is that the cooling effectiveness of the film-cooling flow can be improved by actively controlling (e.g. forcing, pulsing) the jet flow globally or locally, and that active control can be applied to prevent/delay lift-off, selectively suppress mixing and increase lateral spread of the cooling jet. Towards this end, a literature survey was carried out during the second part of the study, covering recent work on film-cooling and transverse jet flows, which are the building block of the film-cooling process. The knowledge and insights gained from this literature survey contributed to the formulation of transverse jet flow-control strategies and the design of a proof-of-concept experiment. The flow-control strategies were identified on the basis of present fundamental understanding of physical mechanisms, such as those contributing to the formation and strength of the counter rotating vortex pair, jet lift-off and cross-flow entrainment. A simulation was carried out of a simplified cold, two-dimensional wall-jet flow to demonstrate in principle the feasibility of effectively controlling mixing between the jet and the free stream as well as the transport near the wall. The simulation was based on a three large-scale-structure mode model superposed on the mean flow of the wall jet, which is spatially evolving downstream. The formulation method employed was an energy integral method commonly used in non-linear stability analysis of shear flows. The results of the simulation showed that mixing and skin friction on the wall can be effectively controlled (reduced or increased) through forcing of the large-scale-structure modes at appropriately chosen initial amplitudes and phases. Upon invoking the analogy between momentum transport and heat transfer it was concluded in principle that both mixing and wall heat transfer can be locally reduced through appropriate global forcing of the wall jet. Feasibility was also reinforced by results of studies that achieved similar objectives through passive means (i.e. geometry modifications), by recognizing that the same effects responsible for the success of such passive means can be achieved through fluidic actuation.

A survey was also conducted of the state of the art in high-temperature micro-sensors (temperature and heat flux), actuators, electronics, communications and materials that

are necessary components of an integrated active film-cooling control system. It was concluded that off-the shelf technology can be used for the proof-of-concept system under cold conditions, while state-of-the art, bench-tested technology would be sufficient for a warm (500C) demonstration system provided that it is further developed and integrated with the specific film cooling application requirements in mind. Substantial development in the relevant areas mentioned above and in materials technology will be needed for the long-term implementation of the system in a realistically harsh environment. Resistive elements integrated using thin film deposition technology were identified as appropriate temperature/heat-flux sensors, and micro-jet terminated acoustic circuits (self-excited or driven by piezoceramic elements) were identified as good actuator candidates. Electronics based on SiC technology and wire harnesses based on thin film technology were deemed appropriate for the application, while a "very-short-range" telemetry system was conceptually laid out for passing signals and power from component to component in the modular environment of the application.

The conclusion of the present investigation is that the concept of an actively controlled film-cooling system is both a useful and feasible one, requiring substantial development for realization. The study culminated into the formulation of a multidisciplinary proposal for the development and demonstration of an actively controlled film cooling system for gas-turbine engine applications. This proposal was submitted to NASA's Revolutionary Aeropropulsion Concepts (RAC) Project of the Aerospace Propulsion and Power Program (Research and Technology Base) and involved participation and collaboration between six branches of the NASA Glenn Research Center (5530, 5520, 5510, 5820, 5120, and 5130).

Name: **Jeremiah E. Oertling**
Status: Undergraduate Student
Institution: Louisiana State University

Accompanying Student under the direction of Professor Dimitris E. Nikitopoulos.

Research Summary Submitted by Student

Toward the Active Control of Heat Transfer in the Hot Gas Path of Gas Turbines

My time at NASA this summer has focused on assisting my Professor's project, namely "Toward the Active Control of Heat Transfer in the Hot Gas Path of Gas Turbines." The mode of controlling the Heat Transfer that the project focuses on is film cooling. Film cooling is used in high temperature regions of a gas turbine and extends the life of the components exposed to these extreme temperatures. A "cool" jet of air is injected along the surface of the blade and this layer of cool air shields the blade from the high temperatures. Cool is a relative term. The hot gas path temperatures reach on the order of 1500 to 2000 K. The "cool" air is on the order of 700 to 1000 K. This cooler air is bled off of an appropriate compressor stage.

There have been two projects that I have worked on this summer. First, I conducted a literature survey of previous studies on film cooling and jets in cross-flow. Second, the Controls Division acquired a 12" x 12" wind tunnel. I was asked to design a modification to this wind tunnel so as to conduct experiments relevant to film cooling.

The Literature survey conducted was started at Louisiana State University. I began collecting journal articles using search parameters given to me by my Professor and continued the process using the facilities at NASA. My first searches included the subject of film cooling, which is a well-documented subject. These papers investigate the aerodynamic phenomena and the heat transfer associated with the jet in cross-flow. The focused turned to a "jet in cross-flow" as I continued to search. These papers, most of which were written before the subject of film cooling had become a widely used form of cooling parts in a turbine, focused solely on the Aerodynamic characteristics of a jet in cross-low. The jet in cross-flow is a problem not solely associated with film cooling. Other areas they are used in are chimneys, V-STOL aircraft, and combustor mixing to name a few. The challenge was to identify the papers that would be relevant to the study of film cooling.

In an effort to identify papers that would pertain to the current study, I was asked to read and classify each article I had found. I read each article and recorded the methods by which the experimenters classified their jet in cross-flow and a host of many of the aspects of the studies. I created an Excel file to store all of my findings. The entries were arranged so that each article could be identified by the parameters that were investigated and the testing equipment used. The summary could be used to easily reference other papers that would pertain to the study. Some of the major aspects of each paper that were the blowing ratio, which is a ratio of the mass flux per unit area of the jet over the mass flux per unit area of the free-stream, the length scale of the jet or jets, the number and arrangement of the jets, and the orientation of the jet.

In recording and classifying these studies, I both provided a condensed version of these papers to my professor and familiarized myself with the terms and concepts of film cooling. Knowing how studies were conducted in the past helped prepare me for my second project that I worked on, designing the test section for the studies to be conducted here.

The wind tunnel manufacturer, GDJ Inc., provided a wind tunnel that will be used by the Controls Division for use on some of their projects. The original test section dimensions were 12" x 12" x 36". The original equipment included an airfoil, balance, a series of pressure taps, and a digital control unit. The tunnel was located in the Advanced Controls and Simulation Laboratory, a computer lab. Due to safety hazards, the tunnel is not allowed to run in the computer lab. Future plans have the tunnel located in building 5 in a test cell. Its current location is building 50, the fabrication shop. I had it sent there to be modified for the elongated test section, which will be explained shortly.

The aim is to actively dissipate the mixing and reduce the vertical injection of the cooling jet. In order to do this, the basic aerodynamics of the jet in cross-flow and the heat transfer associated with the cooling jet need to be characterized. The wind tunnel available to us will allow this testing to take place.

The test section currently being made has the same cross sectional area as the original but has a feature that allows the top wall to be moved. This allows the flow's acceleration to be modified to maintain a zero pressure gradient. The flow naturally accelerates because of the boundary layer growth and the additional mass flow of the jet being injected into the cross-flow. In addition to the movable top wall, the length was increased to 4'. The additional length will allow the far field affects such as span-wise spread of the jet, wake patterns, and vortex structures to be studied.

The next parameter of interest is the jet's position and orientation in the flow-field. The span-wise coordinate is located along the centerline. The symmetry of this location allows an angled hole, regardless of its compound angle, to be located at the centerline. The stream-wise location was chosen because of the relationship to the boundary layer at that location. The boundary layer thickness is approximately 90% of D, the jet diameter, at a location of 30*D, 15 inches. This value of the boundary layer is only an estimation using experimental values for boundary layer estimation. This distance was also in correlation with the studies on film cooling found during the literature survey.

Knowing the location of the hole and the overall test section dimensions, design drawings were made and sent out for estimation. The job was assigned to the fabrication shop, and at the final date of my summer fellowship, the small parts of the test section were being made. My mentor has promised pictures of the final product.

In closing I would like to thank Dr. Dimitris E. Nikitopoulos for the opportunity to join him in his study, Dennis Culley for his guidance during my stay at NASA Glenn Research Center, and University Programs for making it possible to gain this experience.

Name: **Janche Sang**
Education: Ph.D., Computer Science
Purdue University

Permanent Position: Associate Professor, Computer and Information Science
Cleveland State University

Host Organization: Computing and Interdisciplinary Systems Office
Colleague: 2900/Gregory J. Follen

Assignment:

Aviation Safety Modeling and Simulation (ASMM)
Propulsion Fleet Modeling

Within NASA's Aviation Safety Program, NASA GRC participates in the Modeling and Simulation Project called ASMM. NASA GRC's focus is to characterize the propulsion systems performance from a fleet management and maintenance perspective by modeling and through simulation predict the characteristics of two classes of commercial engines (CFM56 and GE90). In prior years, the High Performance Computing and Communication (HPCC) program funded, NASA Glenn in developing a large scale, detailed simulations for the analysis and design of aircraft engines called the Numerical Propulsion System Simulation (NPSS). Three major aspects of this modeling included the integration of different engine components, coupling of multiple disciplines, and engine component zooming at appropriate level fidelity, require relatively tight coupling of different analysis codes. Most of these codes in aerodynamics and solid mechanics are written in Fortran. Refitting these legacy Fortran codes with distributed objects can increase these codes reusability. Aviation Safety's modeling and simulation use in characterizing fleet management has similar needs. The modeling and simulation of these propulsion systems use existing Fortran and C codes that are instrumental in determining the performance of the fleet. The research centers on building a CORBA-based development environment for programmers to easily wrap and couple legacy Fortran codes. This environment consists of a C++ wrapper library to hide the details of CORBA and an efficient remote variable scheme to facilitate data exchange between the client and the server model. Additionally, a Web Service model should also be constructed for evaluation of this technology's use over the next two-three years.

Research Summary Submitted by Fellow:

A Tool for Semi-Automatic Construction of CORBA-based Applications from Legacy Fortran Programs

Components are the computational building blocks of an NPSS Model[1]. Based on the space where they are built, NPSS components can be classified as either internal or external. Internal components can be added by writing C++ code, compiling and linking it into NPSS. For adding an external component, it is necessary to implement the

CorbaExtElement interface which is pre-defined in the NPSS CORBA IDL. Our CORBA-based Wrapping and Coupling Environment supports two families of classes: *ForeignComponent* and *RemoteServer*[2]. The former implements the *CorbaExtElement* interface to plug into NPSS and hides the details of CORBA and IDL interfaces from application developers. The latter encapsulates methods of setting and getting variable defined in the *ForeignComponent* to realize a remote variable scheme. The purpose of the remote variable scheme is to provides a simple and elegant data-sharing capability in the client-server platform. Furthermore, through the operator overloading, the remote variables can be used in much the same way as traditional variables.

The *ForeignComponent* class provides an Application Programming Interface (API) with which the legacy Fortran code can be connected. Programmers need to add the following three routines for wrapping their Fortran application:a startup routine called *NPSS_main* which replaces the *program* statement as the entry point, an initialization routine called *NPSS_initialize* which initializes the NPSS interface an registers remote variables, and a computation routine called *NPSS_execute* which executes the simulation. The variable which the client will access should be registered using a character-string name as the key. For example, the following function:

NPSS_registerReal4Ref('PTI',PTI, PSS_INPUT,NPSS_PUBLIC,'psia','pressure',err)

can be invoked to register the variable *PTI* with the string *'PTI'*as the key . To access this variable in the server CSPAN, programmers have to declare

RemoteReal PTI = RemoteReal(CSPAN,"PTI"); using the same string "PTI" in the client.

In this summer project, we have developed a graphical user interface (GUI) tool to assist programmers in wrapping legacy Fortran codes. Programmers can simply click on a variable from a list box. Corresponding codes related to variable registration in the server and variable declaration in the client can be generated automatically. Hence, tedious programming tasks for wrapping the codes can be greatly reduced. Our GUI-based tool (see Figure 1) which is implemented in Tcl/tk consists of three phases as described below:

Phase I: Check Fortran program structure and extract common/namelist variables

As mentioned earlier, the Fortran program to be wrapped should use *NPSS_main* to replace the normal *program* statement. This phase firstly checks whether the Fortran program has been re-structured to meet the wrapping requirements. Secondly, it extracts the common and namelist variables with their declared types from the Fortran program. These variables are the candidates for being chosen as the remote variables in the next phase. Note that a common variable, e.g. x(50), can appear in several declaration statements:

```
integer  x, a(10), b, c
dimension  x(50), y(20)
common  /cblk/ x,y
```

To accomplish the two tasks mentioned above, we implemented a parser by modifying an existing Fortran-to-C converter called f2C[3]. We utilized the parse tree constructed by the f2c program to generate the following information into an intermediate file:

```
cblk integer  x(50)
```

cblk real y(20)

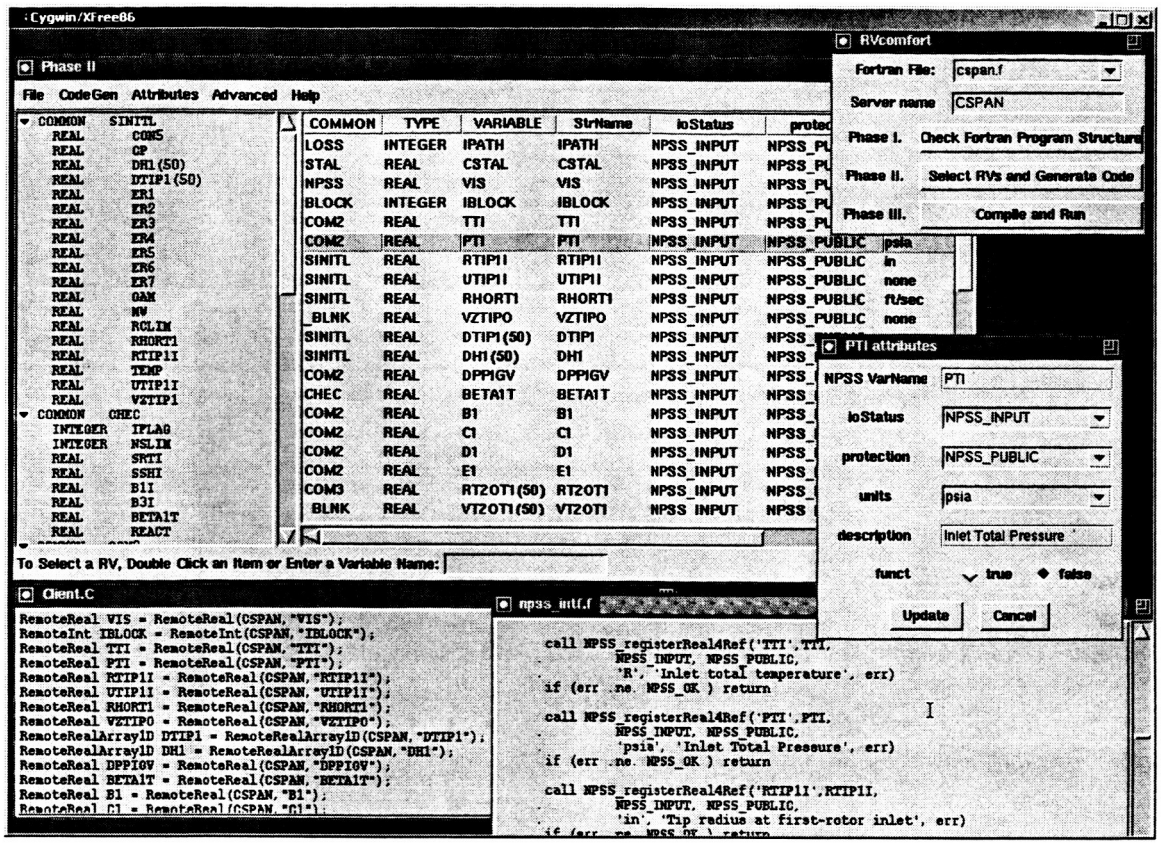

Figure 1 A GUI-based Tool

Phase II: Select remote variables and generate code

The most tedious work using our wrapping environment is to pick up the remote variables and make the corresponding declarations in the server (i.e. the file *npss_intf.f*) and in the client (i.e. the file *Client.C*). We provide a list box to make the selection task easier. Furthermore, each variable has it's own attributes, including I/O status (*NPSS_INPUT* or *NPSS_OUTPUT*), protection (*NPSS_PUBLIC* or *NPSS_PRIVATE*), units, description and a Boolean flag funct. Programmers can change these attributes through a popup window with several pull-down lists and entry boxes. After all necessary variables are selected, the codes will be generated automatically into the file *npss_intf* and the file *Client.C*. Note that if a variable is located in other process (e.g. the MPI worker process), the flag func has to be set to true. The tool will generate the code to register a callback routine for this variable in the server. When the client tries to access this variable, the registered callback routine will be invoked to contact the MPI worker process for getting its value. The advanced options allow programmers to choose repeated executions, server shutdown, interface registration, etc. Figure 1 contains a main phase control window (top-right), a selection window (middle), an attribute-editing window (middle-right), and two windows to display the generated codes (bottom).

Phase III: Compile and run

In the last phase, the tool will create the makefile by inserting the corresponding file names and the CORBA server name into a makefile template. Using the generated makefile, it can compile and build the CORBA server and the client. A test run will be started and the results will be displayed in a window.

Future Work

Currently, the tool generates the code to initialize the remote variable through hardcoded assignment statement (e.g. CP = 1.23;) based on the values stored in the original Fortran namelist input data file. This will generate a lot of assignments and the file *Client.C* will be re-compiled for different namelist file. To solve this, we are planning to implement a class in C++ which can support the Fortran namelist capability. For example,

```
RemoteReal CP    = RemoteReal(cspan, "CP");
RemoteReal MW    = RemoteReal(cspan, "MW");
RemoteRealArray1D SRTIP  = RemoteRealArray1D(cspan, "SRTIP");
RemoteRealArray1D SSH    = RemoteRealArray1D(cspan, "SSH");

# we provide a NameList class, and the tool generate the code below
NameList  Name = CP, MW, SRTIP, SSH};

# through overloading, we can
ifstream   in("fan.input);
in >> Name;
```

It reads the Fortran namelist data file *fan.input* to initialize the variables CP, MW, SRTIP and SSH.

References:

[1] NASA Glenn Research Center, NPSS Component Developer's Guide

[2] G. Follen, C. Kim, I. Lopez, J. Sang, and S. Townsend. A CORBA-based Distributed Component Environment for Wrapping and Coupling Legacy Scientific Codes, Cluster Computing, Vol. 5, Issue 3, 277-285, July 2002.

[3] S. I. Feldman, D. M. Gay, M. W. Maimone, and N. L. Schryer, A Fortran-to-C Converter, Technical Report No. 149, Bell Laboratories, NJ, 1995,

Name: **Theodore J. Sheskin**
Education: Ph.D., Industrial Engineering & Operations Research
Pennsylvania State University

Permanent Position: Professor, Industrial Engineering
Cleveland State University

Host Organization: Power and On-Board Propulsion Technology Division
Colleague: 5450/Raymond F. Beach

Assignment:

Development of Management Metrics for Research and Technology

Professor Ted Sheskin from CSU will be tasked to research and investigate metrics that can be used to determine the technical progress for advanced development and research tasks. These metrics will be implemented in a software environment that hosts engineering design, analysis and management tools to be used to support power system and component research work at GRC. Professor Sheskin is an Industrial Engineer and has been involved in issues related to management of engineering tasks and will use his knowledge from this area to allow extrapolation into the research and technology management area. Over the course of the summer, Professor Sheskin will develop a bibliography of management papers covering current management methods that may be applicable to research management. At the completion of the summer work we expect to have him recommend a metric system to be reviewed prior to implementation in the software environment. This task has been discussed with Professor Sheskin and some review material has already been given to him.

Research Summary Submitted by Fellow:

Development of Management Metrics

The objective of this 2002 summer faculty research assignment was to investigate metrics that can be used to evaluate the progress of technology research and development projects. Two different models are proposed for selecting a project from a set of independent alternative projects. The first model is a modification of one by Meade and Presley ("R&D Project Selection Using the Analytic Network Process," *IEEE Transactions on Engineering Management*, vol. 49, no. 1, pp. 59-66, Feb. 2002) which utilizes the analytic hierarchy process (AHP) developed by Thomas L. Saaty (*The Analytic Hierarchy Process: Planning, Priority Setting, Resource Allocation*. New York: McGraw-Hill, 1980). The second is a decision tree based on the secretary problem which is an example of an optimal stopping problem. The AHP model uses pairwise comparisons to generate metrics. The decision tree model uses pairwise comparisons to calculate probabilities of success. These probabilities and estimated cash flows are used to calculate expected values for the decision tree model. While either model should be satisfactory by itself, developing both models in parallel and attempting to reconcile different outcomes will strengthen the confidence of the decision makers in the credibility of the models. Both models can be implemented on spreadsheets. In

addition, Expert Choice is a software package designed for the AHP. A variety of software tools will create decision trees. Tree Plan is a decision tree add-in for spreadsheets. A small example problem was solved using the AHP model, and a partial decision tree was drawn. The next step is to construct detailed models appropriate for the specific technology R & D projects to be evaluated.

Name: **Ana V. Stankovic**
Education: Ph.D., Electrical Engineering
University of Wisconsin - Madison

Permanent Position: Assistant Professor, Electrical & Computer Engineering
Cleveland State University

Host Organization: Power and On-Board Propulsion Technology Division
Colleague: 5450/Barbara H. Kenny

Assignment:

Simulation, Model Verification and Controls Development of Brayton Cycle PM Alternator

Professor Stankovic will be developing and refining Simulink based models of the PM alternator and comparing the simulation results with experimental measurements taken from the unit. Her first task is to validate the models using the experimental data. Her next task is to develop alternative control techniques for the application of the Brayton Cycle PM Alternator in a nuclear electric propulsion vehicle. The control techniques will be first simulated using the validated models then tried experimentally with hardware available at NASA.

Research Summary Submitted by Fellow:

Testing and Simulation of 2 KW PM Generator with Diode Bridge Output

Testing and simulation of a 2KW PM synchronous generator with diode bridge output is described. The parameters of a synchronous PM generator have been measured and used in simulation. Test procedures have been developed to verify the PM generator model with diode bridge output. Experimental and simulation results are in excellent agreement.

INTRODUCTION
Permanent magnet synchronous generators have tremendous potential in many applications such as wind power generation, solar dynamic power generation as well as in aerospace and marine.

In aerospace applications, high speed is required to minimize volume and weight of a PM synchronous generator.

This work presents the simulation and testing of 2KW, high speed generator, with diode bridge output. The diode bridge output supplies the Ion Thruster in the spacecraft.

SIMULATION AND EXPERIMENTAL RESULTS
Standard procedure has been used to measure the parameters of the 2KW PM generator in the laboratory. The measured parameters have been compared to the

manufacture data and used in simulation. SIMULINK with the Power System Block has been used to simulate the dynamic performance of the PM generator.

Since the generator-turbine shaft has not been accessible the following procedure has been used to verify the generator model.

1. The 2KW synchronous generator, driven by the air turbine, under no load conditions running at 52000 rpm has suddenly been connected to the balanced three-phase resistive load.
2. Generator current, voltage and speed have been recorded in the laboratory.
3. The same procedure has been simulated by using SIMULINK with the Power System Blockset and compared with the experimental results.

As a next step a diode bridge, that supplied a resistive load, has been connected to the output of the PM generator as shown on Fig.1.

With the PM generator conditioned as shown on Fig.1, terminal waveforms for heavy-load conditions have been captured in the laboratory. The same operating point has been simulated by using SIMULINK. Simulation and experimental results are in good agreement.

Due to the dramatic change in harmonic content of both generator voltage and current, additional analysis has to be performed to determine the efficiency of the overall system.

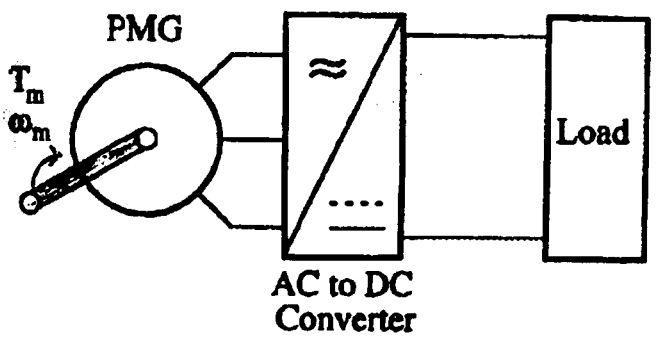

Fig.1

CONCLUSION

The testing and simulation of the 2KW, high speed, PM generator with a diode bridge has been described. Experimental and simulation results are in excellent agreement.

Name: **Thomas M. Ticich**
Education: Ph.D., Physical Chemistry
University of Wisconsin - Madison

Permanent Position: Associate Professor, Chemistry
Centenary College of Louisiana

Host Organization: Microgravity Science Division
Colleagues: 6711/Daniel L. Dietrich
6711/NCMR/Randall L. Vander Wal

Assignment:

Optical and Probe Diagnostics Applied to Reacting Flows

We plan to explore three major threads during the fellowship period. The first interrogates the flame synthesis of carbon nanotubes using aerosol catalysts. Laser light scattering will reveal changes in particle size at various heights above the burner. Analysis of the flame gas by mass spectroscopy will reveal the chemical composition of the mixture. Finally, absorption measurements will map the nanotube concentration within the flow.

The second thread explores soot oxidation kinetics. Cavity ring-down absorption measurements of the carbonaceous aerosol can provide a measure of the mass concentration with time and, hence, an oxidation rate. Spectroscopic and direct probe measurements will provide the temperature of the system needed for subsequent modeling.

The third thread will explore the details of turbulent flame dynamics. Laser induced incandescence will be applied to measurements of soot volume fraction in a 2-d configuration. Analysis of seed tracer particles by planar laser light MIE scattering will reveal the elemental fuel mixture fraction in the flames. Cavity ring-down spectroscopy, a pulsed transient absorption method, will determine the instantaneous mass loading and its fluctuation. Finally, fluorescence measurements will investigate the formation of PAH's in these flames.

Research Summary Submitted by Fellow:

My work this summer focused largely on developing new methods of carbon nanotube synthesis in flames. In particular, we used the technique of *ex-situ* laser ablation to prepare the catalyst and then entrain it into a flame that provided the carbon source, high temperature and appropriate chemical environment to grow carbon nanotubes. The synthesis of carbon nanotubes is an active area of research due to their potential application in molecular-sized circuits, composite materials, hydrogen storage and scanning microscope tips. The most common methods of synthesis to date are by arc-discharge, chemical vapor deposition and laser-ablation of a composite metal target in a high temperature furnace. All of these techniques provide the carbon source, high temperature and appropriate chemical environment to grow carbon nanotubes.

However, they are not readily scalable because they are batch processes that are expensive to carry out. Flames readily provide the high temperature and carbon source in an energy efficient manner and already have demonstrated scalability for other processes. Once supplied with a catalyst, they can serve as a suitable environment for carbon nanotube growth.

During previous summers, I have contributed to the development of several methods of flame synthesis of carbon nanotubes. In particular, we have had success with catalyst preparation and entrainment by organometallic sublimation, spray-pyrolysis of a metal salt solution and thermal evaporation of a metal. One drawback of these techniques is the transient nature of the catalyst entrainment process. A scalable process will be most efficient if run continuously. Therefore, we explored the feasibility of catalyst preparation by laser ablation for subsequent entrainment into a flame to catalyze carbon nanotube growth. The flame was supported on a modified McKenna burner with a center tube. The post-combustion gases of a premixed acetylene/air flame on the burner together with the metal aerosol and other gases added through the center tube provided the nanotube growth environment. Material from the flame was collected on a grid by thermophoretic sampling for subsequent TEM analysis.

We tested two catalyst metals (Fe and Ni), two center tube gas mixtures (A-H_2,He, CO and B-H_2,(He),CO, C_2H_2) each at two different flow conditions, and two equivalence ratios in the acetylene/air flame (1.55 and 1.6). The Fe nanoparticles readily catalyzed the formation of single-wall carbon nanotubes (SWNT's) in both gas mixtures tested. The Ni nanoparticles did not produce SWNT's under any of the conditions. Rather, they formed hollow carbon nanofibers with gas mixture B under conditions with a greater flow of H_2 and CO in the center tube. Other conditions produced large sintered metal particles encapsulated with carbon. Since Fe produced SWNT's under all conditions, it provided the best test for the effect of equivalence ratio and flow rate. Results show that a higher equivalence ratio provides a slightly heavier coating of amorphous carbon which typically dots the SWNT's. The flow rates for mixture B that include lower amounts of H_2 and CO resulted in SWNT's with an extremely heavily coat of amorphous carbon. Hydrogen is known to assist in etching amorphous carbon from diamond film studies and is likely to serve a similar function in our flame environment over a range of concentrations.

The results can be interpreted in terms of the chemical properties of Fe and Ni during CO or C_2H_2 chemisorption. Fe is known to dissociatively adsorb CO at lower temperatures than Ni. Metal and adsorbate form a donor-acceptor bond in which an essentially non-bonding molecular orbital on the carbon atom donates electron density into empty d-orbitals on the metal while filled d-orbitals on the metal donate electron density into an anti-bonding orbital of CO, thereby weakening the C-O bond. The metal-adsorbate bond is stronger for Fe, which has more empty d-orbitals to enable the "donor" portion of the bond. Photoelectron spectroscopy experiments even show that the donation includes a contribution from a bonding orbital in CO. Fe is also known to chemisorb C_2H_2 more strongly than Ni. A donor-acceptor bond is likewise involved in this interaction, although the donor portion involves a bonding orbital for both metals. Hence, C_2H_2 is easier to chemisorb than CO and thus enables nanostructure growth

with the less reactive metal, Ni. Fe presumably chemisorbs C_2H_2 as well but this apparently does not interfere with and may even enhance SWNT growth.

Thus, we have demonstrated the viability of catalyst preparation by *ex-situ* laser ablation for the flame synthesis of carbon nanotubes. These results continue to support the fact that carbon nanotubes can be synthesized in less than 100 ms in a chemically complex environment, as supplied by the flame. (This upper limit for growth time stems from the temperature dependent buoyant acceleration in the flame.) Our work here will also provide an important point of comparison for efforts to improve the spray-pyrolysis method.

Name: **Benjamin F. Pierce**
Status: Undergraduate Student
Institution: Centenary College

Accompanying Student under the direction of Professor Thomas M. Ticich.

Research Summary Submitted by Student

Metal Nonoparticle Catalysts for Carbon Nanotube Growth

My work this summer involved and new and unique process for producing the metal nanoparticle catalysts needed for carbon nanotube (CNT) growth. There are many applications attributed to CNT's, and their properties have deemed them to be a "hot spot" in research today. Many groups have demonstrated the versatility in CNT's by exploring a wide spectrum of roles that these nanotubes are able to fill. A short list of such promising applications are: nanoscaled electronic circuity, storage media, chemical sensors, microscope enhancement, and coating reinforcement.

Different methods have been used to "grow" these CNT's. Some examples are laser ablation, flame synthesis, or furnace synthesis. Every single approach requires the presence of a metal catalyst (Fe, Co, and Ni are among the best) that is small enough to produce a CNT. Herein lies the uniqueness of my work. I used microemulsions (containing inverse micelles) to generate these metal particles for subsequent CNT growth.

A micelle is a grouping of particles in a sphere-like configuration where each particle has a polar head and a non-polar tale, and the polar heads are on the outer region of the sphere. An example of this would be an oil-in-water emulsion. The polar heads would be dissolved in the outer water environment (for water is polar), and the inner core of the sphere would be the non-polar oil bead (with the non-polar tales dissolved in the oil). An inverse micelle is basically a "flipped" micelle. An example is a water-in-oil emulsion. The non-polar tales are on the outer circumference, and the polar heads are dissolved in the inner core.

When these inverse micelles are generated on an extremely small scale, then they serve as "nanoreactors" for the production of these metal nanoparticles because their sizes are contained within the core of the inverse micelle. All of my experimental procedures have involved the reduction of a metal salt (in aqueous solution) to the corresponding metal particle (Cu(s), Co(s), Ni(s), FePt(s), FeOH(s), Fe_2O_3(s), Mo(s) are among some of the metals produced) within an organic environment (non-polar; also including surfactants, which are necessary components of any sort of emulsion). Once this metal salt was reduced, the solution was applied to a substrate (quartz, Cu, Mo, SiC fiber, C fiber, SS mesh, Ni mesh, Al/Mg mesh are among some of the substrates used) in some fashion. The choice of substrate is extremely important due to the strong interactions between the substrate and the metal products, which then alters the catalytic properties of the metal. Once proper application is achieved, the substrate is placed in a tube furnace for CNT growth using the Chemical Vapor Deposition (CVD) method. The tube furnace has a mixture of inert gases, hydrogen gas, and a

hydrocarbon gas flowing through its tube at such a temperature that the carbon from the hydrocarbon gas is deposited onto the sample. If the metal and substrate is an appropriate match, the result is CNT growth. Analysis was made via scanning electron microscopy (SEM) or transmission electron microscopy (TEM) images, courtesy of Lee J. Hall and Dave Hull respectively.

The goal of my summer work was basically to accomplish as much preliminary work as possible. I strived to pinpoint which variable (experimental process, metal product, substrate, method of application, CVD conditions, etc.) was the determining factor in the results. The resulting SEM images were sufficient for the appropriate comparisons to be made. The future work of this project consists of the optimization of the more promising experimental procedures and further exploration onto what exactly dictated the results.

Name: **Fuqin Xiong**
Education: Ph.D., Electrical Engineering
University of Manitoba

Permanent Position: Associate Professor, Electrical and Computer Engineering
Cleveland State University

Host Organization: Communications Technology Division
Colleague: 5650/Kue S. Chun

Assignment:

Professor Xiong will investigate robust synchronization schemes for dynamic channel environment. A sliding window will be investigated for symbol timing synchronizer and an open loop carrier estimator for carrier synchronization. Matlab/Simulink will be used for modeling and simulations.

Research Summary Submitted by Fellow:

Robust Synchronization Schemes for Dynamic Channel Environments

Introduction and Acknowledgements
My tenure at NASA Glenn research center is from May 20 to August 16, 2002, with a 3-week break in between. My host is Mr. Kue Chun of ORG. Code 5650, Digital Communications Technology Branch, Space Electronics Division. My major research is robust symbol timing synchronization techniques for AATT program at NASA GRC.

The NASA colleagues at 5650 have been helping me and collaborating with me on my research topics. Without their help, collaboration, and inspiration, the accomplishments I have achieved in this short period of time are impossible. I would like to thank all colleagues of 5650 Branch. Particularly, I would like to thank the Branch Chief, Mr. Gene Fujikawa, for his leadership, Mr. Kue Chun for his sponsorship and collaboration in synchronization research and Dr. Romanofsky of branch 5640 for his sponsorship and collaboration in the modulation study project.

The mutual understanding of our research interests and goals established during this Summer Fellowship Program will definitely benefits all of us in years to come. I am looking forward to having more collaboration with my NASA colleagues in the future.

Major Accomplishments

1. Robust Synchronization Techniques for CDMA for the AATT Program
   The modem of the AATT mobile Ku-Band earth station developed by NASA GRC is an EB200 spread spectrum modem manufactured by L-3 Corporation. It has experienced communication outages during tests, when the mobile unit passes under highway overpasses or shadowed by other obstacles. The outages are most likely caused by loss of synchronization. The research is to find the exact cause of the outage and to develop robust synchronization techniques for the CDMA modem.

A graduate student, Stanley Pinchak, and I have been working on the project. Mr. Kue Chun, my host of the summer fellowship and the sponsor of the robust synchronization technique project, has been collaborating with me. The project started last summer, continued in this summer and will continue for 2 to 3 years. During this summer's 10-week period, significant progress has been achieved. A robust symbol-timing scheme called sliding window symbol timing synchronizer has been devised, analyzed, and simulated. In particular, the phase detector characteristic has been analyzed. Based on the phase detector characteristic, a sliding window averager and a control algorithm have been devised. Simulation was performed to confirm the phase detector characteristic and to check the phase lock performance. Simulation results show that the synchronizer can work for QPSK at signal-to-noise ratio (Eb/No) as low as –3dB, with a near zero phase error. The convergence time for the phase error to fall in the tolerance of half sampling period is in the neighborhood of 100 symbols. Further research is needed to improve the performance, particularly, to shorten the convergence time and to lock onto incoming signals with not only phase difference, but also frequency offset.

2. Phase Transient Analysis of the Reflectarray Antenna's Phase Shifters

   There was some progress made on the modulation study for the reflectarray antenna for the Power Efficient Reflectarray Communication System (PERCS) being developed at NASA Glenn Research Center. The modulation study started last summer and has achieved its major goal of intersymbol interference analysis and simulation. A remaining task is the study of the antenna performance during the transient period when the antenna is switching from one direction to another. Dr. Romanofsky of the RF Applied Technology Branch, who is the principal investigator of the reflectarray and the sponsor of the modulation study project, has been collaborating with me on this phase transient study. We have had several in depth discussions about this. Both he and I have had MathCAD programs for calculating the phase transient behavior of the antenna. No final conclusions have been made. The research is in progress.

3. Papers: An article titled "Sliding Window Symbol Timing Synchronizer" (12 printed pages) has been written based on the research results and submitted to 21st Digital Avionics Systems Conference (DASC), Irvine, California, 27-31 October 2002.

4. Other Tasks Completed:
   Served as consultant on several issues:

   a) Discussed with Marc Seibert of Digital Communications Technology Branch and his student intern Michelle on error control coding techniques for his photon image transmission and reception system. Recommended the (7,4) Hamming code and explained it to Michelle.

Reviewed and commented on a CICT proposal synopsis titled "Development of adaptable, high throughput digital communication technology for direct access of a user to a satellite" draft by Kue Chun.

References and Notes

(i) Meador, M. A. B.; Johnston, J. C.; Cavano, P. J.; Frimer, A. A. *Macromolecules* **1997**, *30*, 3215-3223.

(ii) Meador, M. A. B.; Johnston, J. C.; Frimer, A. A.; Gilinsky-Sharon, P. *Macromolecules* **1999**, *32*, 5532-5538.

(iii) Meador, M. A. B.; Lowell, C. E.; Cavano, P. J.; Herrera-Fierro, P. *High Perform. Polym.* **1996**, *8*, 363-379.

(iv) (a) Meador, M. A. B.; Johnston, J. C.; Hardy-Green, D.; Frimer, A. A.; Gilinsky-Sharon, P.; Gottlieb, H.E. *Chemistry of Materials,* **13**, 2649-2655 (2001); (b) Meador, M. A. B.; Frimer, A. A. "End Caps Increase Thermo-Oxidative Stability of Polyimides," *NASA Tech Briefs*, October 2001, LEW-16987. This paper was awarded a NASA Certificate of Recognition for Technical Innovation. (c) Meador, M. A. B.; Frimer, A. A. "Polyimides and Process for Preparing Polyimides Having Improved Thermal-Oxidative Stability," U.S. Patent Number 6,303,744, October 16, 2001.

(v) Alston, W.B. personal communication (August 2002) regarding unpublished results.

(vi) St. Clair, A. K.; St. Clair, T. L. *Polym. Eng. Sci.* **1982** *22*, 9-14.

(vii) The butadienes are commercially available, with the exception of *trans*-1-phenylbutadiene: Grummit, O.; Becker, E.I. *Org. Synthesis*, Coll. Vol. **IV**, 771 (1963).